(2)

NAVAL POSTGRADUATE SCHOOL
Monterey, California

AD-A207 896

THESIS

FLIGHT TEST METHOD DEVELOPMENT FOR A
QUARTER-SCALE AIRCRAFT WITH
MINIMUM INSTRUMENTATION

by

Nicolaos D. Bamichas

March 1989

Thesis Advisor: Richard Howard

UNCLASSIFIED

SECURITY CLASSIFICATION OF THIS PAGE

REPORT DOCUMENTATION PAGE

1a REPORT SECURITY CLASSIFICATION UNCLASSIFIED	1b RESTRICTIVE MARKINGS
2a SECURITY CLASSIFICATION AUTHORITY	3 DISTRIBUTION/AVAILABILITY OF REPORT Approved for public release; distribution is unlimited
2b DECLASSIFICATION/DOWNGRADING SCHEDULE	
4 PERFORMING ORGANIZATION REPORT NUMBER(S)	5. MONITORING ORGANIZATION REPORT NUMBER(S)
6a NAME OF PERFORMING ORGANIZATION Naval Postgraduate School 6b OFFICE SYMBOL (If applicable) 67Ho	7a. NAME OF MONITORING ORGANIZATION Naval Postgraduate School
6c. ADDRESS (City, State, and ZIP Code) Monterey, California 93943-5000	7b. ADDRESS (City, State, and ZIP Code) Monterey, California 93943-5000
8a. NAME OF FUNDING/SPONSORING ORGANIZATION 8b. OFFICE SYMBOL (If applicable)	9. PROCUREMENT INSTRUMENT IDENTIFICATION NUMBER
8c. ADDRESS (City, State, and ZIP Code)	10. SOURCE OF FUNDING NUMBERS PROGRAM ELEMENT NO. / PROJECT NO. / TASK NO / WORK UNIT ACCESSION NO.

11. TITLE (Include Security Classification)
FLIGHT TEST METHOD DEVELOPMENT FOR A QUARTER-SCALE AIRCRAFT WITH MINIMUM INSTRUMENTATION

12. PERSONAL AUTHOR(S)
BAMICHAS, NICOLAOS

13a. TYPE OF REPORT	13b. TIME COVERED	14. DATE OF REPORT (Year, Month, Day)	15. PAGE COUNT
Master's Thesis	FROM ______ TO ______	1989 March 23	80

16. SUPPLEMENTARY NOTATION
The views expressed in this thesis are those of the author and do not reflect the official policy or position of the Department of Defense or U.S. Govt.

17. COSATI CODES			18. SUBJECT TERMS (Continue on reverse if necessary and identify by block number)
FIELD	GROUP	SUB-GROUP	Radio-Controlled Aircraft, Instrumentation, Drag Polar, Thrust Required, Power Required, Flight Test, Wind Tunnel, Torque Stand, Theses. (SDW)

19. ABSTRACT (Continue on reverse if necessary and identify by block number)

A flight test method was developed for a quarter-scale model aircraft with minimum onboard instrumentation for the determination of the Drag Polar, the Thrust Required curve and the Power Required curve. The test included a wind tunnel test for propeller efficiencies and thrust coefficients, a torque test for engine shaft horsepower, and a flight test for flight speeds at measured operating conditions. The only additional onboard instrumentation besides that for radio control was a small cassette recorder. Two methods are described for data manipulation and an error analysis is provided for each method. Keywords:

20 DISTRIBUTION/AVAILABILITY OF ABSTRACT ☒ UNCLASSIFIED/UNLIMITED ☐ SAME AS RPT. ☐ DTIC USERS	21. ABSTRACT SECURITY CLASSIFICATION UNCLASSIFIED
22a NAME OF RESPONSIBLE INDIVIDUAL RICHARD HOWARD	22b TELEPHONE (Include Area Code) (408) 646-2870 22c. OFFICE SYMBOL 67Ho

DD FORM 1473, 84 MAR 83 APR edition may be used until exhausted. All other editions are obsolete

SECURITY CLASSIFICATION OF THIS PAGE

☆ U.S. Government Printing Office: 1986—606-24.

UNCLASSIFIED

Approved for public release: distribution is unlimited.

Flight Test Method Development for a Quarter-Scale Aircraft with Minimum Instrumentation

by

Nicolaos D. Bamichas
Captain, Hellenic Air Force

Submitted in partial fulfillment of the requirements for the degree of

MASTER OF SCIENCE IN AERONAUTICAL ENGINEERING

from the

NAVAL POSTGRADUATE SCHOOL
March 1989

Author: ______________________
Nicolaos D. Bamichas

Approved by: ______________________
Richard Howard, Thesis Advisor

____
Eric Pagenkopf, Second Reader

____
E. Roberts Wood, Chairman,
Department of Aeronautical Engineering

____
Gordon E. Schacher,
Dean of Science and Engineering

ABSTRACT

A flight test method was developed for a quarter-scale model aircraft with minimum onboard instrumentation for the determination of the drag polar, the trust required curve, and the power required curve. The test included a wind tunnel test for propeller efficiencies and thrust coefficients, a torque test for engine shaft horsepower, and a flight test for flight speeds at measured operating conditions. The only additional onboard instrumentation besides that for radio control was a small cassette recorder. Two methods are described for data manipulation and an error analysis is provided for each of the methods.

TABLE OF CONTENTS

LIST OF TABLES

LIST OF FIGURES

TABLE OF SYMBOLS

AR	Aspect Ratio
b	Wingspan
BHP	Brake Horse Power
C_D	Drag Coefficient
C_{Do}	Parasite Drag Coefficient
C_L	Lift Coefficient
C_T	Thrust Coefficient
c_r	Chord at the Root
c_t	Chord at the Tip
d	Propeller Diameter
D	Aircraft Drag
e	Oswald Efficiency Factor
F	Force Measured in Torque Stand
J	Advance Ratio
l	Torque Stand Arm Length
L	Aircraft Lift
mAh	Milliamperes per Hour
N	Revolutions per Second
P	Atmospheric Pressure

P_{iw}	Power Required, corrected for Standard Conditions, Standard Weight
P_r	Power Required
Q	Torque
R	Gas Constant for Air
RPM	Revolutions per Minute
S	Wing Area
T	Thrust
T_r	Thrust Required
T_{corr}	Thrust from Wind Tunnel Test, after correction made for the torque factor
T_{read}	Thrust Reading in Wind Tunnel Test
V	Velocity
V_{iw}	Velocity for Standard Weight, Standard Conditions
V_s	Same as V_{iw}
V_t	Velocity as Obtained from Flight Test
W	Aircraft Weight
w_{CD}	Drag Coefficient Uncertainty
w_{CL}	Lift Coefficient Uncertainty
w_{CT}	Thrust Coefficient Uncertainty
w_J	Advance Ratio Uncertainty
w_P	Power Required Uncertainty

w_T	Thrust Uncertainty
W_s	Standard Weight of the Aircraft
W_t	Test Weight of the Aircraft
w_v	Velocity Uncertainty
σ	Density Ratio
σ_t	Test Density Ratio
ρ	Air Density
ρ_o	Air Density at Sea Level Standard Conditions
ρ_t	Test Air Density
η	Propeller Efficiency
α	Angle of Attack
π	3.1415926
Λ	Sweep Angle
λ	Taper Ratio (c_t/c_r)

ACKNOWLEDGEMENT

I would like to thank Pat Hickey, Jack King and John Moulton for their help during this project. I would like to give special thanks to Don Harvey who built the torque stand and helped to build the aircraft, and to Don Meeks whose 30 years experience in flying radio controlled airplanes, proved to be valuable for the flight test. Special thanks also are deserved by my Thesis Advisor Dr. Richard Howard who helped me to integrate this work.

Finally, I would like to thank my family, my parents and everybody else, who helped me during these past two years at the Naval Postgraduate School.

I. INTRODUCTION

"The unmanned vehicle of today is a technology akin to the importance of radar and computers in 1935." [Ref. 1, p. 12] These are the words with which Dr. Edward Teller, father of the nuclear age, recently referred to remotely piloted vehicles (RPVs).

The success of the Israelis in the Bekaa Valley in 1982, certify the truth of Dr. Teller's words. By flying small RPVs in the Valley, the Israelis destroyed 29 surface-to-air Syrian SAM missiles in one single hour [Ref. 1, pp. 3-4].

This success caused many countries to become interested in RPVs and to start or accelerate RPV programs which have played a major role in the military world in the last few years.

Low risk, due to lack of human beings on board, makes their procurement progress easier. Some, as Pioneer, proceeded without flight test. Therefore, many unknowns may exist about the aircraft's performance.

In this report, a method of flight testing a small radio controlled aircraft was developed. The goal was to develop the drag polar and the power required curves for the aircraft with minimal onboard instrumentation. Instrumentation is very important for small aircraft, where the weight factor is very critical--a one or two pound payload increase can be detrimental.

II. BACKGROUND

Model Airplanes: To dream, to build, and then to fly.

The roots of their art may go back to ancient Egypt, where a small winged object of sycamore was found in 1898 in a royal tomb. Archytas, a contemporary of Plato, is credited with flying a mechanical bird successfully also, around 400 BC. In 1804, Englishman Sir George Cayley fashioned a glider, and in 1871, Frenchman Alphonse Penault built a stable miniature aircraft powered by a rubber band. [Ref. 2, p.132]

At Westover Air Force Base in Chicopee, Massachusetts, the rubber band still powers aircraft in a model competition category called free flight. Two other categories of model aircraft competition are radio control, in which an aircraft responds to signals from a transmitter, and control line, where the builder manipulates a handle whose wires are attached to the airplane. [Ref. 2, p. 132]

Today, the technology of radio control systems advances very fast. Remotely controlled aircraft earn more and more of the interest of people compared to the other two categories. The advanced technology of electronics and the ability of building highly advanced sensors integrated into a small size that can fit in these small airplanes makes them an important weapon from the military point of view.

During the last 20 years, much research for RPVs has been done and many flight tests have been performed.

In 1975, a propeller and engine testing for mini-remote piloted vehicles was performed with wind tunnel and torque stand tests, at the Air Force Institute of Technology at Wright-Patterson AFB.

In 1975, NASA Dryden Flight Research Center flight tested a large-scale (3/8) model of an F-15 fighter aircraft, to investigate the stability and controllability of the configuration at high angles of attack. [Ref. 3, p.1]

The same organization, in 1986, developed an experimental flight test maneuver autopilot for a .44-scale version of an envisioned full-scale fighter aircraft [Ref. 4, p.1], that was designed to increase the quantity of data obtained in flight tests.

In 1976, at a symposium held at the Royal Aeronautical Society in London, "RPVs - Roles and Technology," was discussed in a paper by the British Aircraft Corporation. Since then, research on the "stabilized" RPV has been accomplished within the United Kingdom UMA Systems Research Programme. [Ref. 5, p. 136]

In 1985, five joined wing RPVs were flight tested at North Carolina State University, in order to examine the behavior of these aircraft in flight. [Ref. 6, p. 1]

In 1985, at Mississippi State University, a method was devised to determine the propulsive efficiency and aircraft drag from steady state flight test data. The method used was based on a computer formulation of Lock's equivalent propeller model. [Ref. 7, p. 1]

At the Naval Postgraduate School, a RPV program sponsored by NAVAIR has started. RPV research projects can be used to investigate aerodynamic phenomena of interest to NAVAIR with application to the RPV or to other aircraft.

In 1988, a RPV was designed and its construction started for use in investigating the feasibility of using the Wortmann FX 63-137 airfoil, as well as to improve the stability and control characteristics of the Pioneer RPV.

Also in that same year, two model aircraft were delivered to the Naval Postgraduate School. A half-scale Pioneer RPV, used for training by the U.S. Navy and the U.S. Marine Corps, and a quarter-scale general aviation type aircraft were acquired. The program for these aircraft included flight tests in order to develop their performance in terms of aerodynamic and powerplant characteristics. Wind tunnel tests and measurements of the engine on a torque stand were also accomplished in order to develop a method for flight testing of radio-controlled aircraft.

This report deals with the quarter-scale flight testing and complementary tests. The limited payload capability of this aircraft necessitated minimum onboard instrumentation.

III. EXPERIMENTAL PROCEDURE

The goal of the flight test was to obtain the drag polar of the airplane, and the thrust required and power required curves. To reach that goal, it was necessary to develop the following:

- Variation of the power with RPM and throttle setting
- Variation of the thrust that the propeller produces at various flight speeds
- Variation of the propeller efficiency with the advance ratio

All of the above requirements were obtained by performing three major tests.

First, a torque stand test was accomplished. In this test, the torque of the engine was measured and its power was calculated. By using six different loads, the power versus RPM curves were plotted for various throttle settings.

Using the 3.5' x 5' wind tunnel of the Naval Postgraduate School, the propeller thrust coefficient and efficiency variation with the advance ratio were developed.

Finally, a flight test was performed, in order to collect data for the airplane in flight. These data consisted of the velocity of the aircraft at every engine throttle setting and the RPM.

The method that will be followed to obtain the drag polar and the power required curves, hereafter referred to as thrust method, is as follows:

Manipulating thrust, velocity and RPM data from a wind tunnel test, will provide the C_T versus J plot. Then, from that plot, the thrust in flight will be obtained through the RPM and velocity measured in flight. The drag and Lift coefficients as well as the power required will then be calculated, so that the drag polar and the power required curves can be obtained and plotted.

Another available method to obtain the above results is hereafter referred to as the power method. From the power versus RPM plot, obtained from a torque stand test, and the propeller efficiency versus the advance ratio plot, obtained from a wind tunnel test, the power required and thrust required are calculated and plotted as well as the drag coefficient so that the drag polar is plotted. These methods will be described in more detail in following sections.

A. THE AIRPLANE

The airplane that was used for this flight test was a quarter-scale general aviation type, radio-controlled airplane (Figure 1). Its main components were an aluminum tube, to which were attached the foam-core wings and horizontal tail, the wooden vertical tail, a 3-HP single- cylinder two-stroke gasoline engine and the plastic fuselage. In the plastic fuselage were mounted a 14-ounce fuel tank, the radio receiver, the battery and the four servos for the ailerons, the elevator,

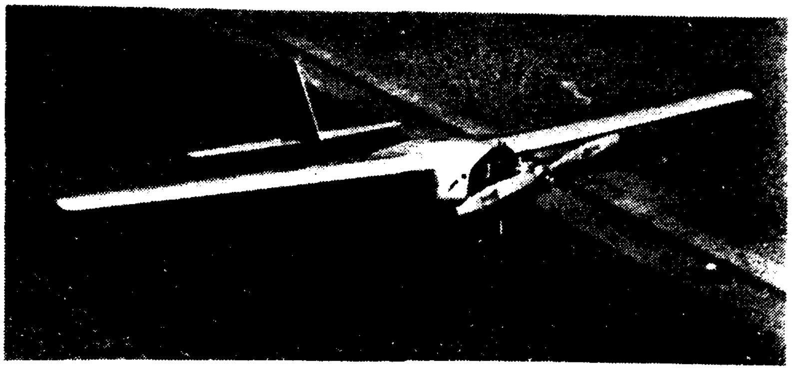

Figure 1A. The Quarter-Scale General Aviation Aircraft

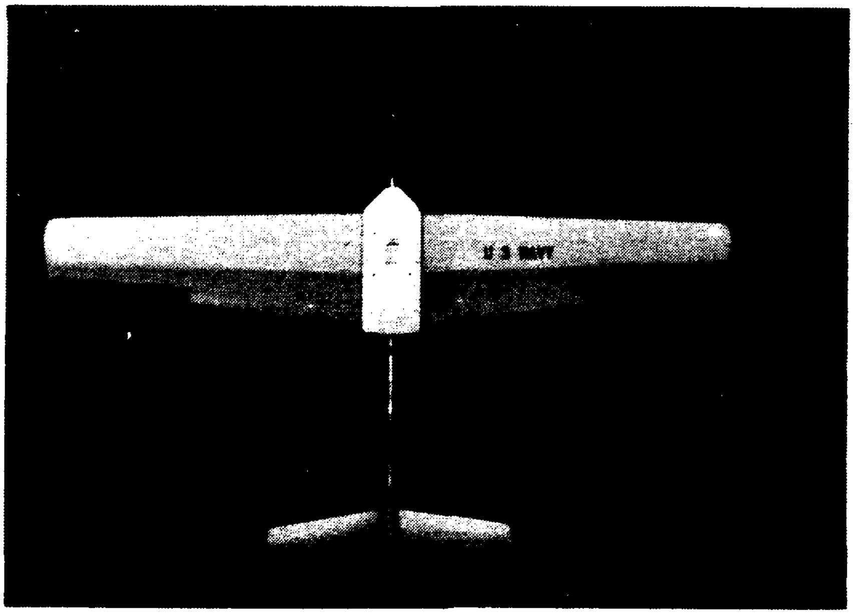

Figure 1B. Top View of the Aircraft

the rudder and steering and the throttle. Mounted to the aluminum tube in the fuselage were the two supports for the wings and the main landing gear.

Before the final adjustment of the push rods for the three control surfaces and the throttle could be made, the wing structure and fuselage were located to set the proper position of the c.g. at approximately 25% chord. Later on, for a known location of the landing gear with respect to the aircraft reference, measuring the weight distribution gave the exact c.g. position. Its variation with fuel consumption was found to be from 26.25 to 27.52% of the aerodynamic chord as shown in Figure 2. Upon completion of the aircraft construction, its geometric parameters were measured. The results are shown in Appendix A.

The engine was a single-cylinder, 40 cc two-stroke gasoline engine, rated at 3-HP at a maximum speed of 11000 RPM.

The propeller that was used for the entire test was a 20-8[1] wooden propeller. Before any tests or flights could be accomplished, break-in of the engine was necessary. To do so, the engine was mounted on a wooden stand made for this purpose. Break-in consisted of two hours total running, at all throttle settings. During break-in, adjustment of the engine was also performed to ensure the best performance at low as well as at high RPM.

[1]20-8 propeller refers to a 20-inch diameter and an 8-inch pitch, the pitch being the distance that the propeller advances in one revolution.

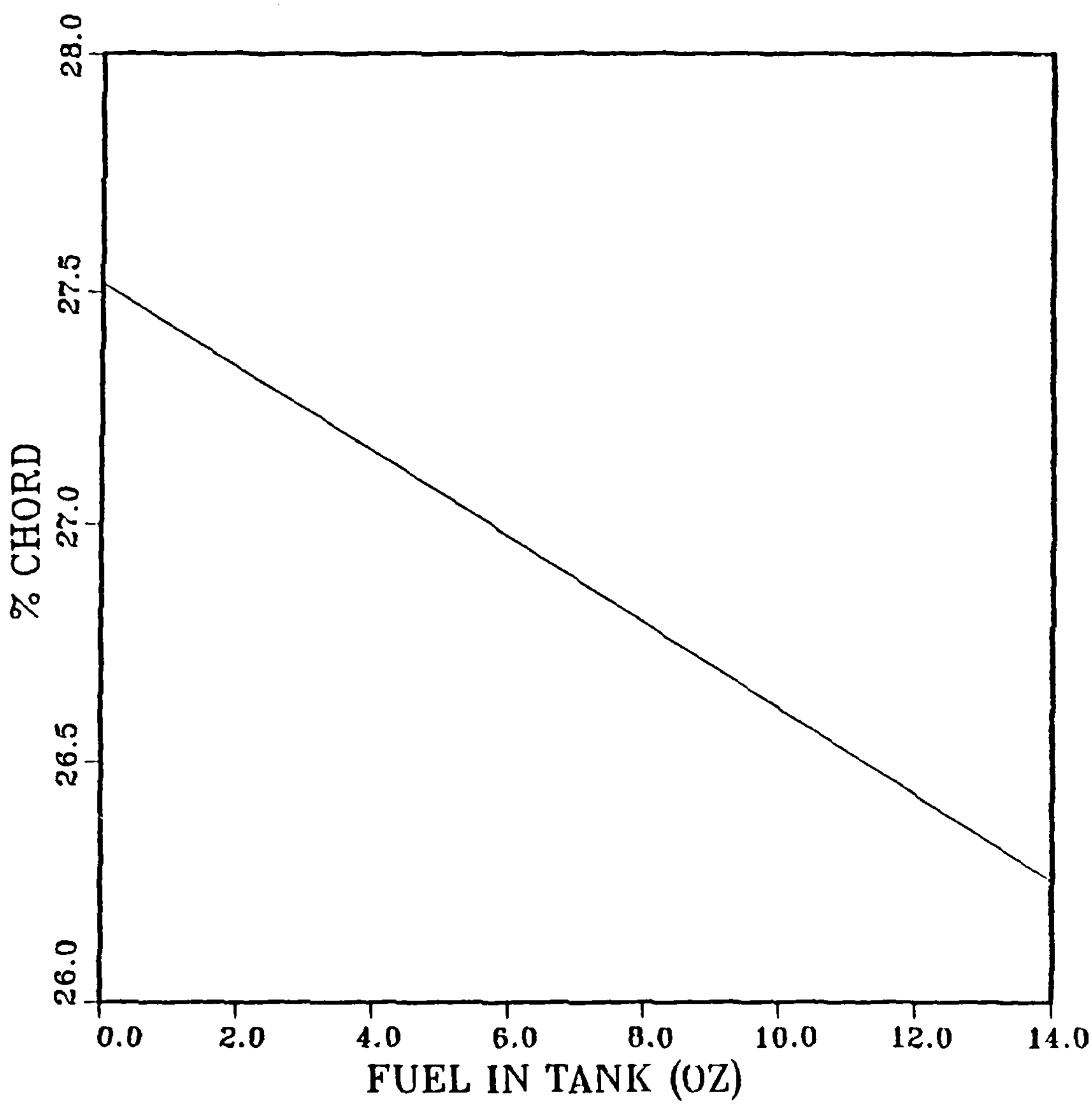

Figure 2. c.g. Variation with Fuel Consumption

B. TORQUE STAND

To measure the Power of an engine vs RPM, three types of devices are commonly used.

The first one is the dynamometer. It consists of an electric generator to which the engine is attached [Ref. 8, pp. 21-22] (Figure 3). When the engine drives the generator at various RPM, the generator delivers electric power. Proper instrumentation converts this electric power to that of the engine being tested. Dynamometers are the most accurate horsepower measuring devices, as well as the most expensive. For such a high RPM engine, an eddy current type (at a cost of approximately $25,000) would be necessary for this test.

The second type of device available to measure the power is the prony brake. The prony brake (Figure 4) [Ref. 8, p. 20] is a simple friction device which, when clamped to the end of the crankshaft, measures the torque or turning moment of the engine. As shown in the figure, the engine is provided with a brake drum and brake blocks to which is attached a torque arm. At the end of the torque arm a scale measures the applied force. The brake is applied and with the engine turning at the desired RPM, the force which is acting on a scale at the end of the torque arm can be measured. Problems of other investigators with the prony brake led to the design and construction of the torque stand [Ref. 9, p. 38].

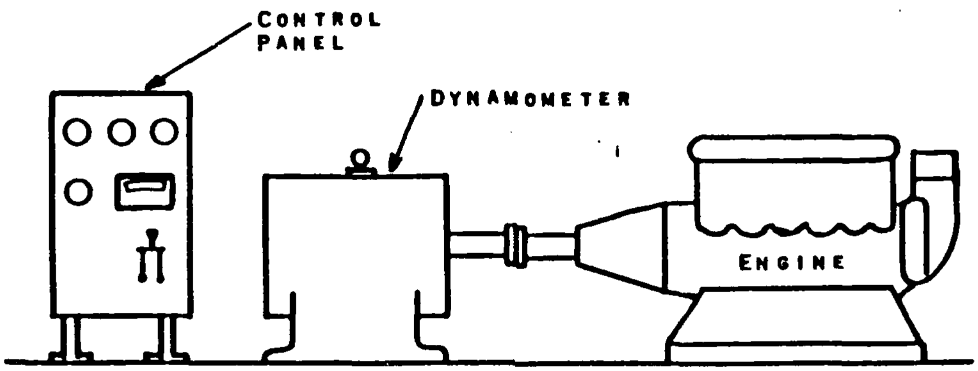

Figure 3. The Dynamometer

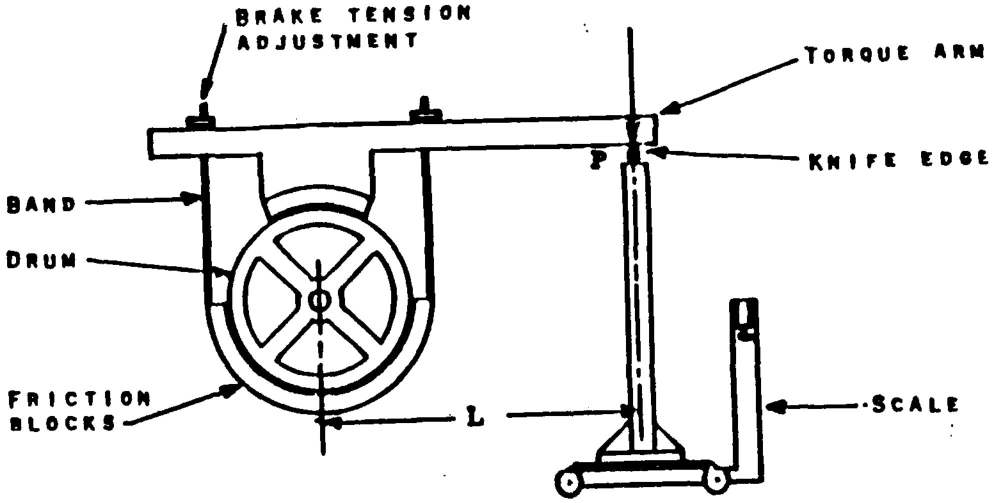

Figure 4. The Prony Brake

The principle of operation of the torque stand is that during operation, the engine exerts a torque. Measurement of this torque permits the calculation of the BHP through the formula:

$$BHP = 2*\pi*l*F*RPM/33000 \qquad \text{(eqn. 3-1)}$$

where

33000 = 550 ft-lb/HP * 60 sec/min from RPM

The torque stand (Figure 5 and Figure 6) was designed by the author and built in the facilities of the Naval Postgraduate School. It consisted of an aluminum plate attached to a steel shaft which, being supported by two bearings, was free to rotate. A torque arm 20 inches long was mounted to the aluminum plate. At the end of this torque arm, a load cell was attached, to measure the force exerting by the engine torque. The measuring device consisted of the load cell, a power supply and a voltmeter. The load cell was a strain gage compression type rated up to 10 lbs. It was connected to a bridge with four input resistances of 350 ohms each. An initial calibration with known weights was performed and an excitation voltage of 6.743 V was found to give scaled linear variation with load. A mechanical scale was used after damage of the load cell due to engine periodic strong vibrations. This mechanical scale was rated up to 25 lb with a 0.01 lb resolution.

In order to determine the horsepower curve, different loads at every engine throttle setting must be used. In this way, a curve of the power versus RPM

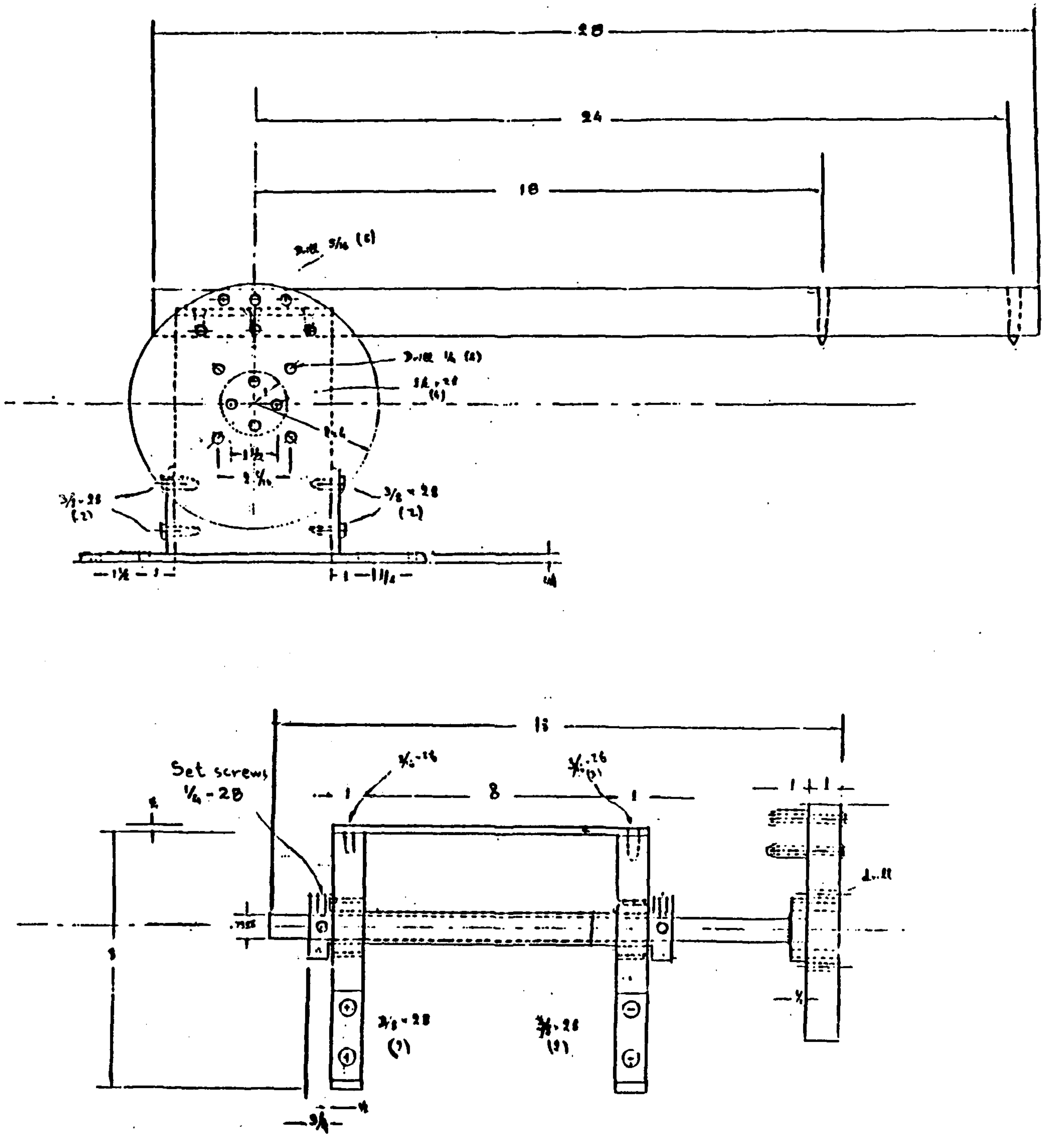

Figure 5. The Torque Stand Design

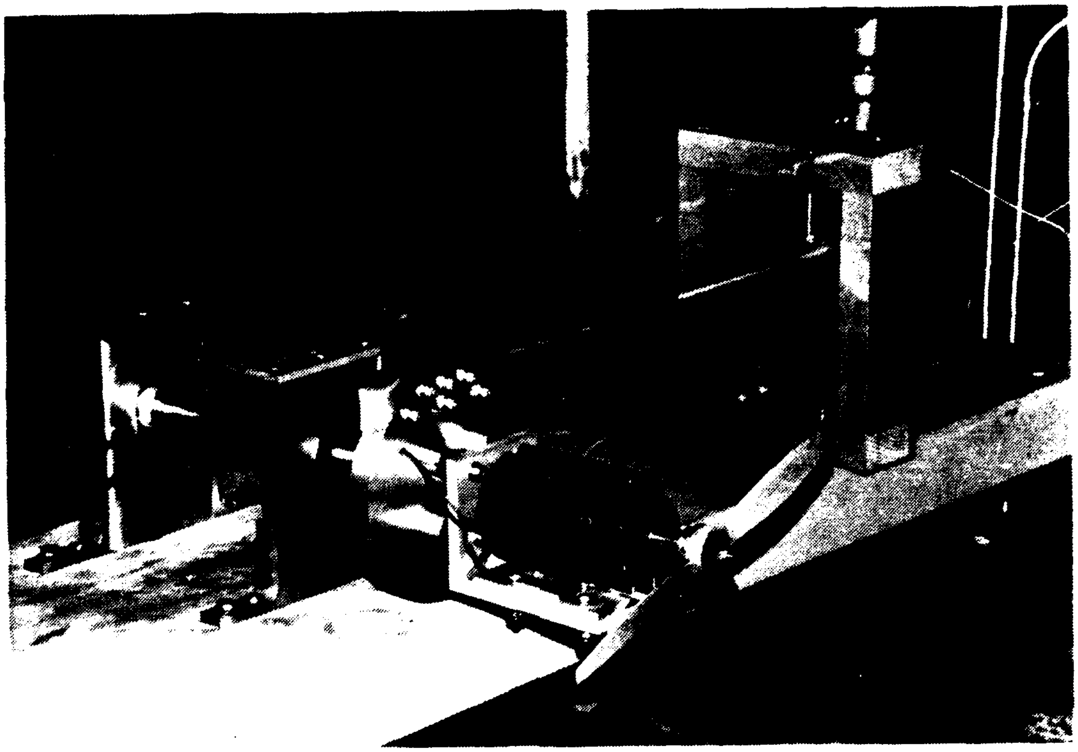

Figure 6. The Torque Stand

can be constructed for every throttle setting. Then, by knowing the RPM at some throttle setting in flight, the brake horsepower can be obtained for that particular configuration. As different loads, six different propellers were used: 20-8, 18-8, 16-8, 14-8, 11-8 and 10-7.

C. WIND TUNNEL

In order for the propeller performance to be determined, i.e., the thrust coefficient and efficiency variation with the advance ratio, a wind tunnel test was necessary. The 3.5' x 5' wind tunnel of the Naval Postgraduate School was used. It is a closed circuit, single return, low speed wind tunnel.

The advance ratio may be interpreted as the distance traveled forward during each propeller revolution (V/N), normalized by the propeller diameter (d) [Ref. 10 p. 9]:

$$J = V/Nd \qquad \text{(eqn. 3-2)}$$

The thrust coefficient is defined as

$$C_T = T/\rho N^2 d^4 \qquad \text{(eqn. 3-3)}$$

Operation of the gasoline engine in the wind tunnel would require the necessity of special construction of an apparatus for collecting exhaust gases, result in difficulty in starting the engine in the limited space of the test section, and create safety problems due to the existence of flammable fuel in the wooden wind tunnel. For the above reasons and because the thrust that the propeller produces depends only on the RPM and flow velocity and is independent of the motor that turns it, an electric motor was used instead of the airplane engine for the thrust tests.

The propeller used in flight was mounted to the electric motor through a shaft adaptor. The electric motor was attached to a thrust stand (Figure 7) designed by Lieutenant James Tanner [Ref. 11]. This thrust stand consisted of an aluminum 18-inch long arm with a window for the attachment of four strain gages to measure the displacement caused by the thrust force. A proper calibration of the stand with known weights, resulted in a voltage reading corresponding to thrust in pounds. A toothed wheel was attached to the motor shaft which in combination with a magnetic proximity sensor attached to the stand, gave the RPM of the propeller. For more information on the thrust stand see [Ref. 11].

A variable voltage source played the role of the throttle by changing the input voltage to the motor from 0 to 140 volts. In this manner the voltage could be varied at a set tunnel speed, and the RPM and the thrust measured, to result in a curve of the thrust coefficient versus the advance ratio.

D. FLIGHT TEST

To test fly the airplane, various methods and techniques exist. The one which will be used depends on what is currently under investigation. In this case, with a small scaled aircraft, the goal was to obtain the drag polar and the thrust required and the power required as functions of flight speed.

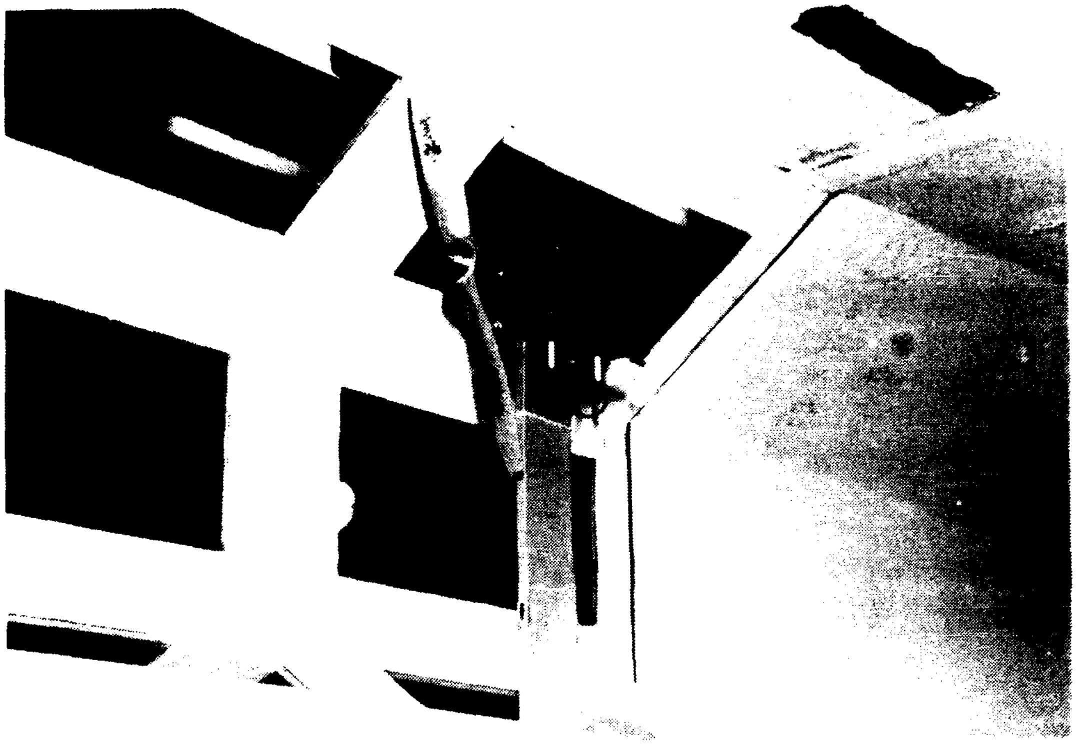

Figure 7. The Electric Motor and the Thrust Stand in the 3.5' x 5' Wind Tunnel

For the drag polar to be calculated, the variables that are necessary to be known are velocity, RPM, and thrust. The lift coefficient in straight and level flight (where Lift = Weight) depends on the weight of the airplane (Figure 8), the dynamic pressure and the wing area, i.e.,

$$C_L = W/qS = W/½\rho V^2 S \qquad \text{(eqn. 3-4)}$$

For known weight and wing area, the only unknown that must be determined is the dynamic pressure, and for measured pressure and temperature, this unknown reduces to the true velocity of the airplane.

To calculate the drag coefficient requires more effort. Since the drag coefficient C_D is defined as:

$$C_D = D/qS = D/½\rho V^2 S \qquad \text{(eqn. 3-5)}$$

drag, as well as velocity, must be known.

Because the flight is straight and level, thrust is equal to drag, i.e.,

$$T = D$$

But from equation (3-3),

$$T = C_T \rho N^2 d^4 \qquad \text{(eqn. 3-6)}$$

In other words, for constant ρ and d, C_T and N must be determined. The thrust coefficient of the propeller vs advance ratio is known from wind tunnel test results. The rotational speed N (or RPM) was recorded in flight onboard the aircraft.

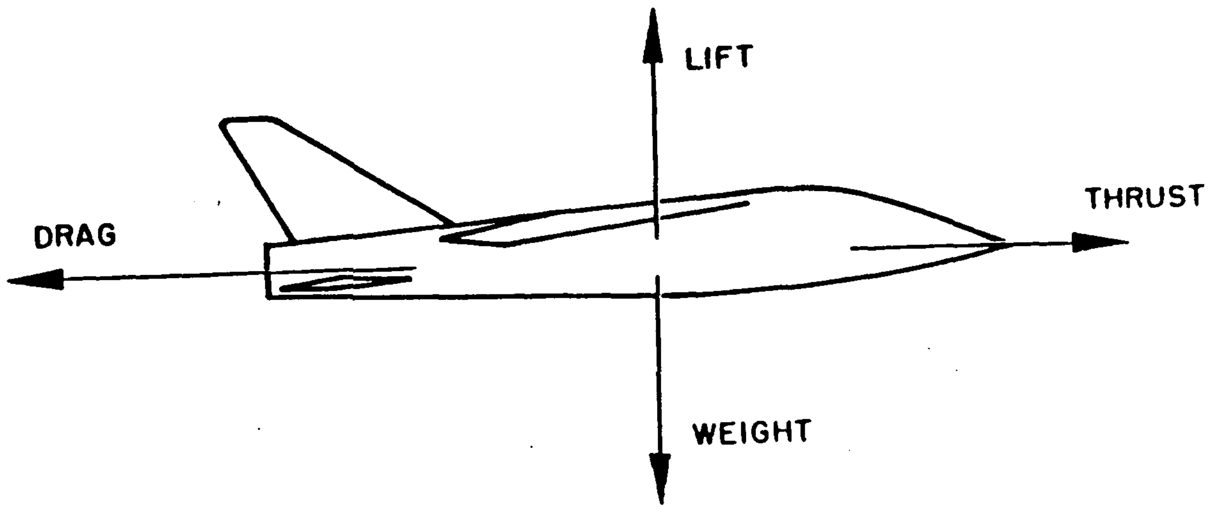

Figure 8. Forces on the Aircraft on Steady Level Flight

To determine true flight speed, the ground speed course method [Ref. 12, p. 4.16] was chosen. This is a method that is used by general aviation aircraft to compute the position error of the pitot static system. The method consists of runs over a premeasured ground distance. By recording the time it takes for the airplane to travel the marked distance, the true Velocity can be calculated. To eliminate the effect of any headwind, two runs in opposite directions must be conducted. By averaging the two velocities, the wind component cancels out with the assumption that it was constant during these two runs. The airplane should also be allowed to drift with the crosswind, i.e., the aircraft should be allowed to fly on the magnetic heading of the ground course so that the crosswind component is eliminated also. Each pair of runs must be accomplished at constant RPM, i.e., constant throttle setting.

To measure the RPM in flight, a small cassette recorder, weighing seven ounces, was mounted inside of the fuselage. A wire was wrapped around the spark plug cable so that a periodic electric signal was transmitted by induction to the recorder through a shielded cable. Playback of the cassette into a frequency counter revealed the frequency of this signal and the RPM of the engine. This cassette recorder was the only onboard instrumentation used in this flight test.

IV. RESULTS - DISCUSSION

A. PRETEST FLIGHT

An introductory flight was necessary after the airplane had been built. The main reason for this is for checkout of any handling problems or trim adjustments. A very experienced pilot must be chosen for this very first flight.

Preflight inspection included:

- Inspection of engine for good condition and to ensure bolt tightness

- Inspection of fuselage for good condition and to ensure tightness of all parts (receiver, battery, servos, etc)

- Inspection of correct movement of all control surfaces and engine throttle

- Range test for the transmitter. A 200 ft test with the transmitter antenna collapsed was positive and guaranteed that a much longer range would be obtained during flight with the antenna extended. This test was accomplished with the engine running, to ensure that there was no interference from the engine. A second range test was conducted during the taxi test.

- Engine operation at different throttle settings and engine response. The engine must run smoothly at 4-cycle operation (low speeds) as well as at 2-cycle operations (high speeds).

- Taxi test--for good response of the airplane and centered nosewheel steering straight taxiing at neutral. A second range test for the transmitter was also accomplished during taxiing.

- Shutdown and inspection of the engine for loose bolts or fittings.

- Fuel tank inspection for good condition.

After the preflight inspection, the first flight was conducted. Tests during this first flight were performed in order to certify:

- Control surface response
- Correct trim of the airplane
- Engine response
- Possible frequency interference for the radio
- Effect of c.g. location
- Speed of the airplane at minimum throttle setting

For this airplane, in accordance with the pilot's recommendations, the required adjustments, after this first flight, were elevator trim adjustment and movement of the c.g. location from 25% chord to 30% chord. This last adjustment was accomplished by adding a small weight behind the c.g. and by moving the recorder to the rear part of the fuselage. On subsequent flights, instead of the weight, a larger battery of 1200 mAh capacity replaced the existing one of 500 mAh. This also gave a longer flight time due to the extra battery life, and eliminated the possibility for electric power loss in flight. A second flight indicated that the addition of the small weight was unnecessary and had an undesirable effect on low speed behavior. A third flight, with the final configuration of the airplane, gave results that promised a safe test flight for the airplane.

B. FLIGHT TEST

The flight test data were collected on two different days. The first day, the flight test took place at Fritzsche Army Airfield, Fort Ord, California. Runs were performed over a premeasured distance of 1500 ft and for throttle settings from 8 to 20[2]. Four persons were used during this flight test to collect the data: the pilot and the person that was timing the runs and recording time, throttle position and run number, standing at the midway point of the ground course; and one person at each end of the ground course, signalling the passage of the aircraft and the beginning of the timing. The time for each run was recorded on a flight test form, specifically designed for this experiment (Appendix B). The ambient temperature and the atmospheric pressure were obtained from the nearest airport. The air density was calculated from the equation of state:

$$\rho = p/RT \qquad \text{(eqn. 4-1)}$$

The RPM were recorded by the cassette recorder mounted in the fuselage of the airplane. In order to provide correspondence between the RPM and each particular run during playback of the cassette, a second recorder synchronized with the one in the airplane, was used. Into this recorder, the person recording the time announced the start and end of each run as well as each throttle setting change.

[2]The throttle lever on the transmitter had 23 settings. These were set up to correspond to throttle openings from 30% to 100%.

Every five to six two-pass runs, the airplane was landed for refueling. An estimation of the fuel consumption was recorded so that the Velocity could be corrected to standard weight by

$$V_s = V_t(W_s/W_t)^{1/2}(\sigma_t)^{1/2} = V_{iw} \qquad \text{(eqn. 4-2)}$$

On that day some frequency interference was observed, causing apparent problems of piloting the aircraft. This interference was considered serious and led to the use of another field, at Los Banos, California, for the second's day flight test.

On the second day of testing, the ground course distance was reduced to 1000 ft due to the limited ground run distance available. The same measurements as for the first day of testing were made, this time for all throttle settings. A new temperature and pressure were also recorded.

After calculation of velocities corrected to standard weight, an average velocity and an average test weight were used for further calculations. Values of these, as well as RPM data, are shown in Table 1.

For each test weight and the corresponding velocity, the lift coefficient was calculated from eqn. 3-4.

C. TORQUE STAND

As mentioned in Chapter III, a torque stand was used to determine the power of the engine at various throttle settings and RPM.

The data recorded are shown in Table 2 and the power curves vs RPM are plotted in Figure 9 for the electric motor. From this plot the BHP of the motor can be obtained for some particular RPM and throttle setting. This value of BHP was used to determine the propeller efficiency from the wind tunnel test data for the same throttle setting.

A large periodic fluctuation of the force reading from the load cell was observed, specifically at high throttle settings. Careful search for the cause of this fluctuation revealed that the flowfield from the propeller blowing on the torque stand was producing a lift to the torque stand arm. The solution to this problem was the installation of a protective panel in front of the arm. As indicated by the electric motor power data, this lift gave an error of as much as 20%.

Unfortunately, due to strong high-frequency vibrations of the aircraft engine, the strain-gage load cell was damaged and a mechanical scale was used in its place. This scale had an resolution of 0.01 pound which was considered very satisfactory for these measurements.

A casting failure in the engine crankcase prevented further measurements of the aircraft engine, with the protective panel installed.[3] Figure 10 shows the power curves plotted without the protective panel. (Comparing the shape of

[3]The consolation of this misfortune was that the torque stand was the last test conducted. All flight test data had been collected when the failure occurred.

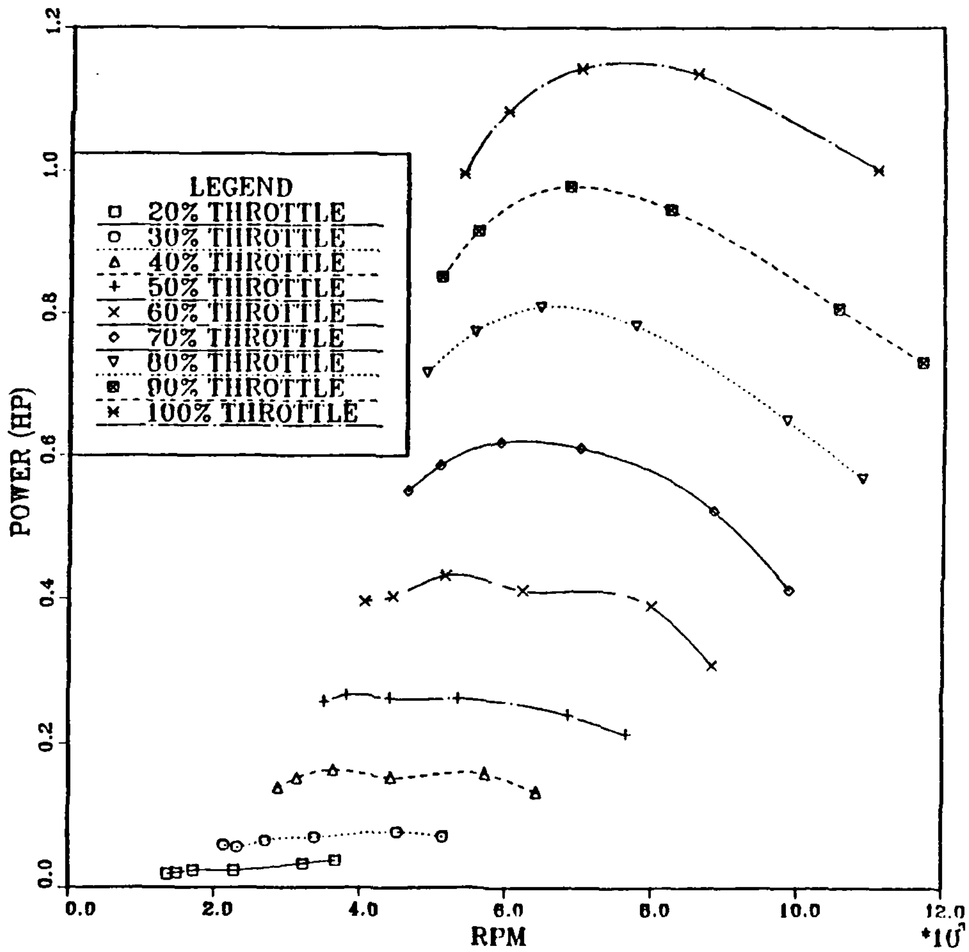

Figure 9. Power Versus RPM

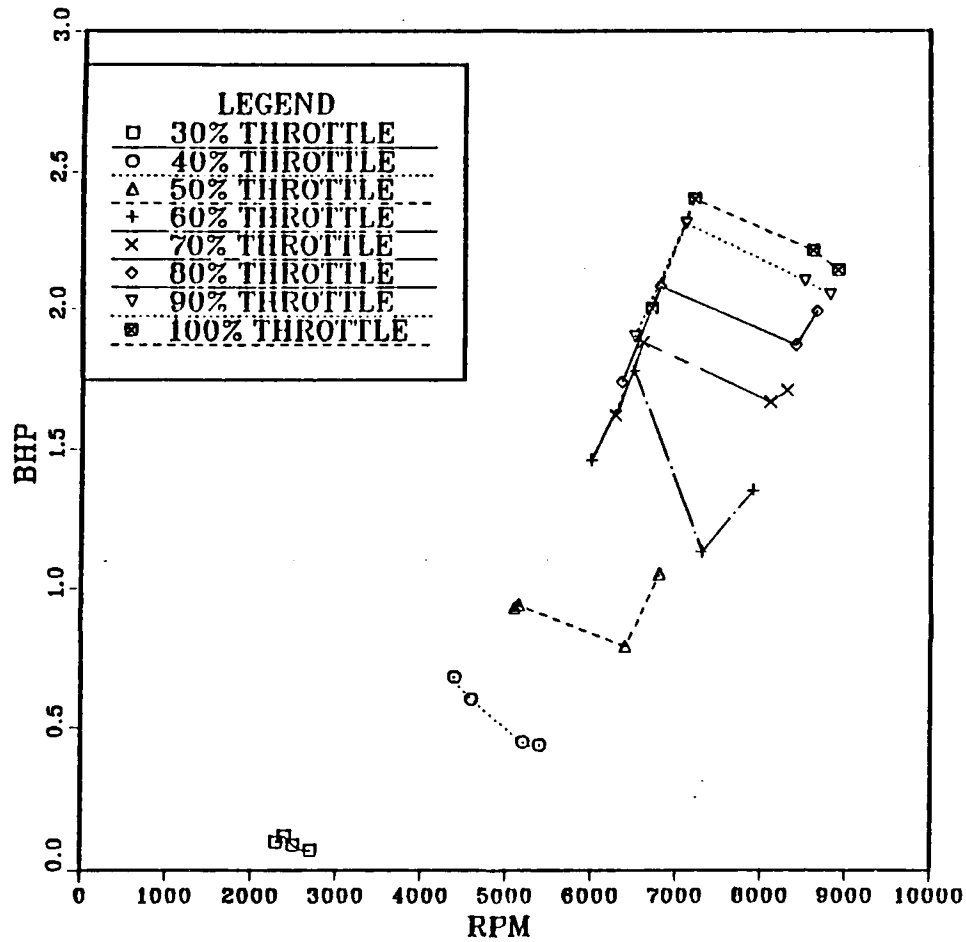

Figure 10. Engine Power Versus RPM

these plots with the one of the electric motor plots, the effect of the flowfield from the propeller can be observed.)

D. WIND TUNNEL

The last set of data was obtained from the wind tunnel test. The temperature and pressure were recorded from the thermometer and barometer of the wind tunnel. The conditions were measured to be T = 63°F and P = 30.38 in Hg. Three runs were performed, at three different wind tunnel velocities of 40.4, 60.06 and 73.67 fps in an attempt to get a wider distribution of J. At each run the thrust and the RPM were recorded for each throttle (or voltage) setting. The results are shown in Table 3. From the reading of the voltmeter for the thrust, a correction was made for engine torque. Specifically, part of the reading was due to the actual torque of the motor. To correct for this, the voltage measured at the torque stand was subtracted from the voltage reading of the wind tunnel so that the corrected thrust corresponds to pure thrust of the propeller.

In accordance with eqn. 3-2 and eqn. 3-3, the advance ratio and the thrust coefficient were calculated (Table 3) and the C_T vs J curve was plotted (Figure 11). To fit the data in this plot, the curve fitting method of least-square regression was used. Looking at this Figure, a considerably large scatter can be observed. One reason for the scatter can be attributed to the electric motor. The 20-8 propeller proved to be a heavy load for this 1-HP motor causing it to

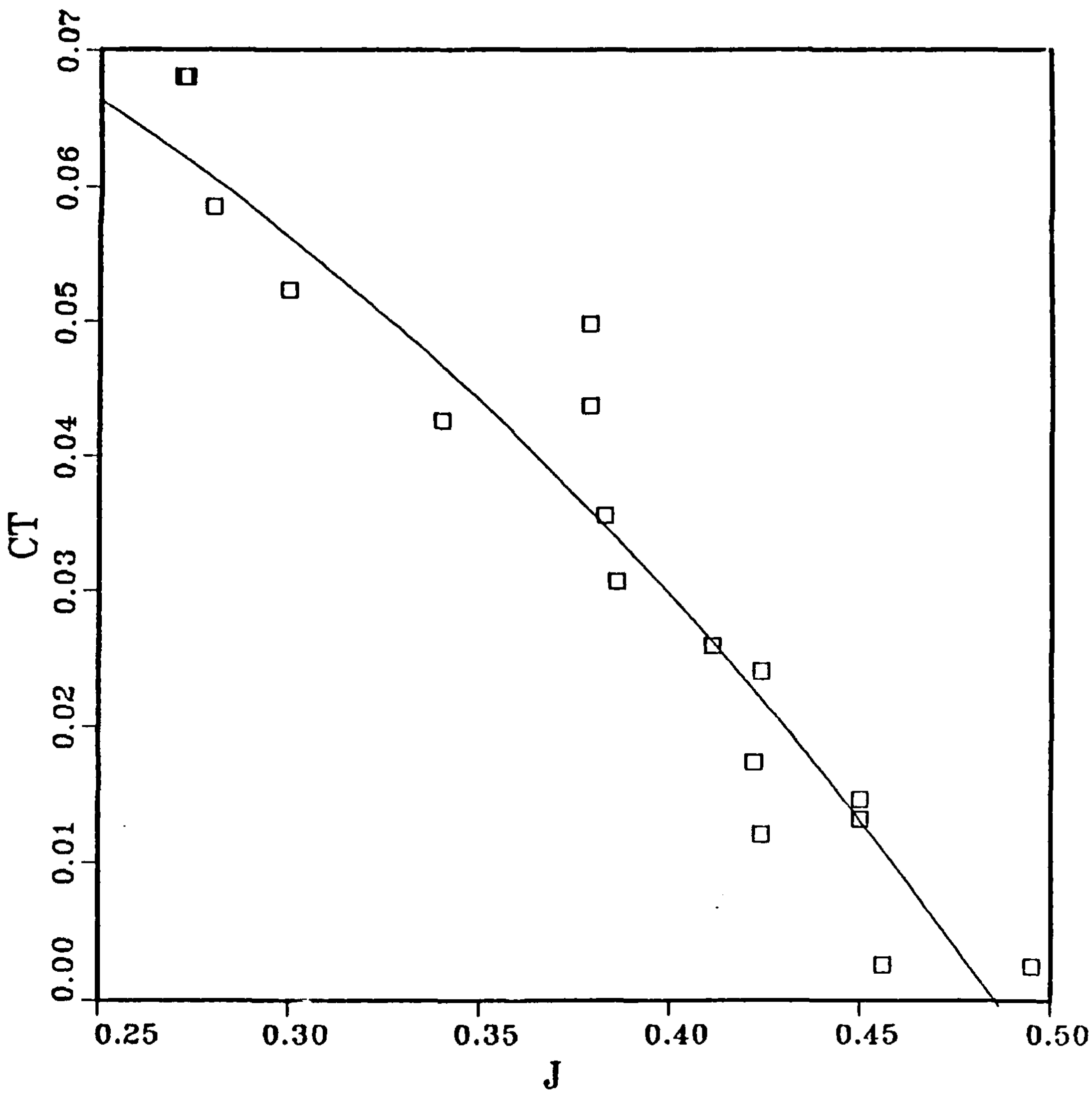

Figure 11. Thrust Coefficient Versus Advance Ratio

overheat, which tended to reduce RPM. To minimize the temperature effect, one to two minute intervals with the electric motor stopped were taken between each throttle setting to allow the engine to cool down by the wind tunnel air flow.

Another reason for the data scatter is due to the error in reading the RPM. At high throttle settings, a significant thrust change corresponded to a very small RPM change, as can be seen in the thrust versus RPM plot (Figure 12). Since in eqn. 3-3 the RPM are squared, the result gives a large scatter for those points. An extended error analysis relating to the scatter is given in Chapter V, Error Analysis. It is considered that more runs at various wind tunnel velocities at throttle settings up to 80% would give more precise data.

The efficiency of the propeller was calculated from the formula

$$\eta = T\ V/BHP\ 550 \qquad \text{(eqn. 4-3)}$$

where BHP was obtained from the BHP versus RPM plot (Figure 9) by entering with the RPM corresponding to each value of thrust T and knowing the throttle setting at which they were obtained in the wind tunnel.

The plot (Figure 13) gives a maximum propeller efficiency of 83% at an advance ratio of about .32 and 0% at 0.495. This reveals that to have best results the aircraft should fly in the advance ratio regime from 0.30 to 0.35. The large scatter that is observed in this plot is attributed to the same causes as for the C_T vs J diagram.

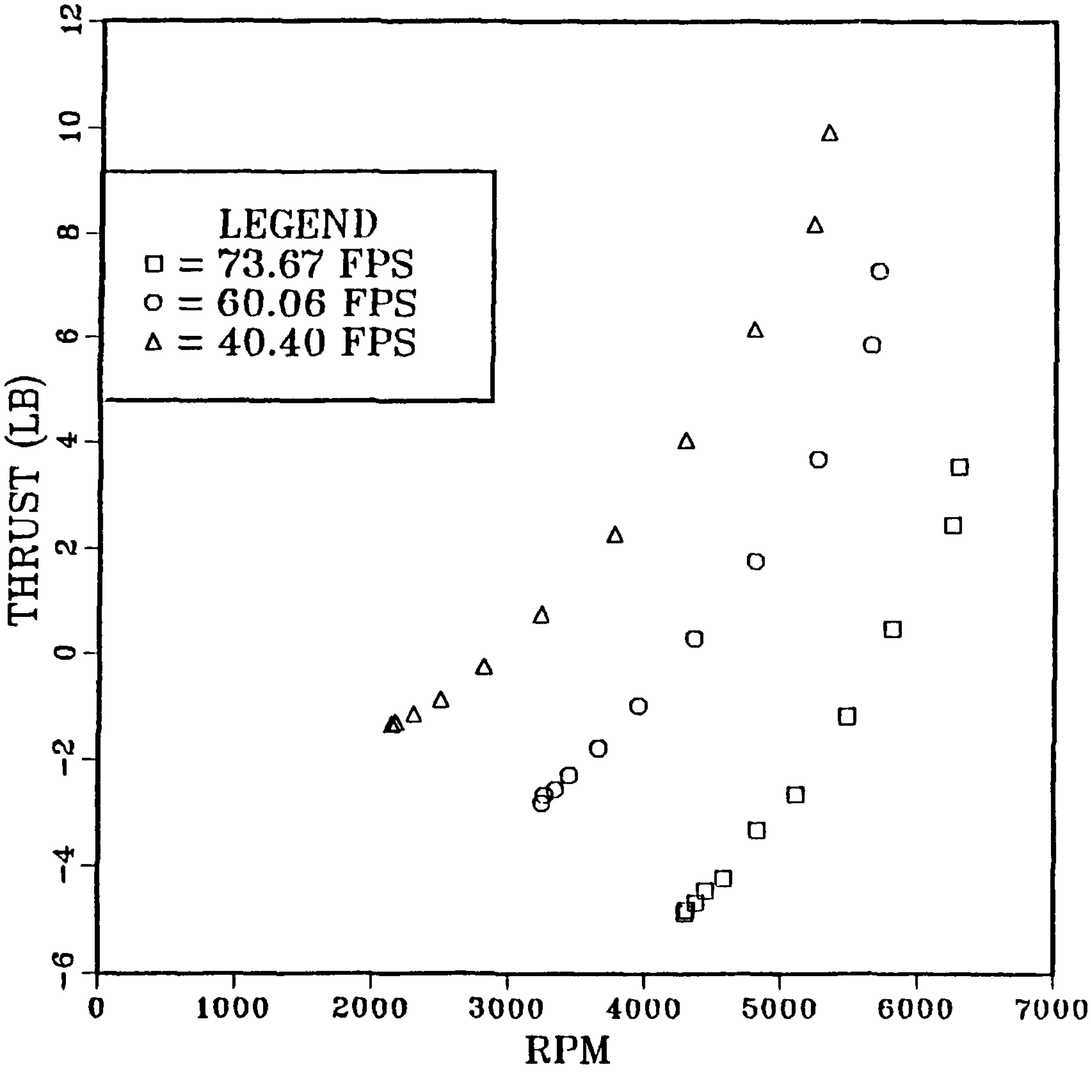

Figure 12. Thrust Versus RPM

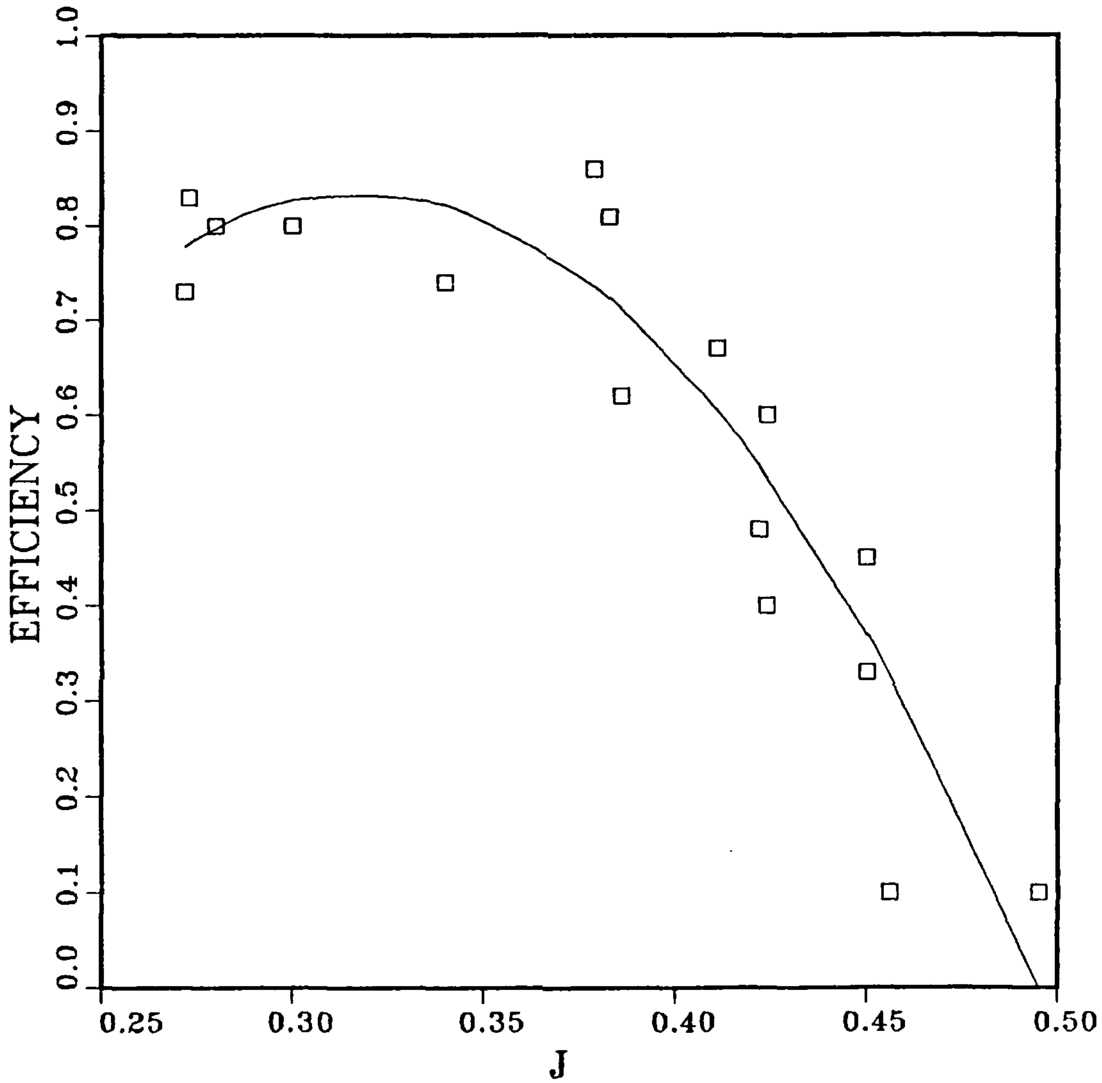

Figure 13. Propeller Efficiency Versus Advance Ratio

The above two curves with the flight test data form the basis for the development of the drag polar, the thrust required and the power required curves.

As shown in Chapter III, C_L can be calculated from eqn. 3-4 and from eqn. 3-5.

Then from eqn. 3-6 the thrust can be calculated as follows:

For a certain velocity from flight test data (Table 1) and the corresponding RPM, the advance ratio can be calculated (eqn. 3-2). Using this advance ratio in the C_T vs J plot (Figure 11), the thrust coefficient is obtained. Then from eqn. 3-6, the thrust can be calculated and from eqn. 3-5, the drag coefficient.

Since the drag polar equation can be assumed to be parabolic [Ref. 13, pp. 211-215] of the form

$$C_D = C_{Do} + C_L{}^2/\pi eAR \qquad \text{(eqn. 4-4)}$$

If C_D is plotted versus $C_L{}^2$, the resulting line should be straight, based on the parabolic assumption. By curve-fitting those data (Figure 14), the drag polar equation is obtained (as shown in Figure 15):

$$C_D = .045 + .0640C_L{}^2 \qquad \text{(eqn. 4-5)}$$

From the drag polar equation, the parasite drag coefficient has a value of

$C_{Do} = .045$

and from $1/\pi eAR = .0640$ the Oswald efficiency factor is found to be

$e = 0.69$

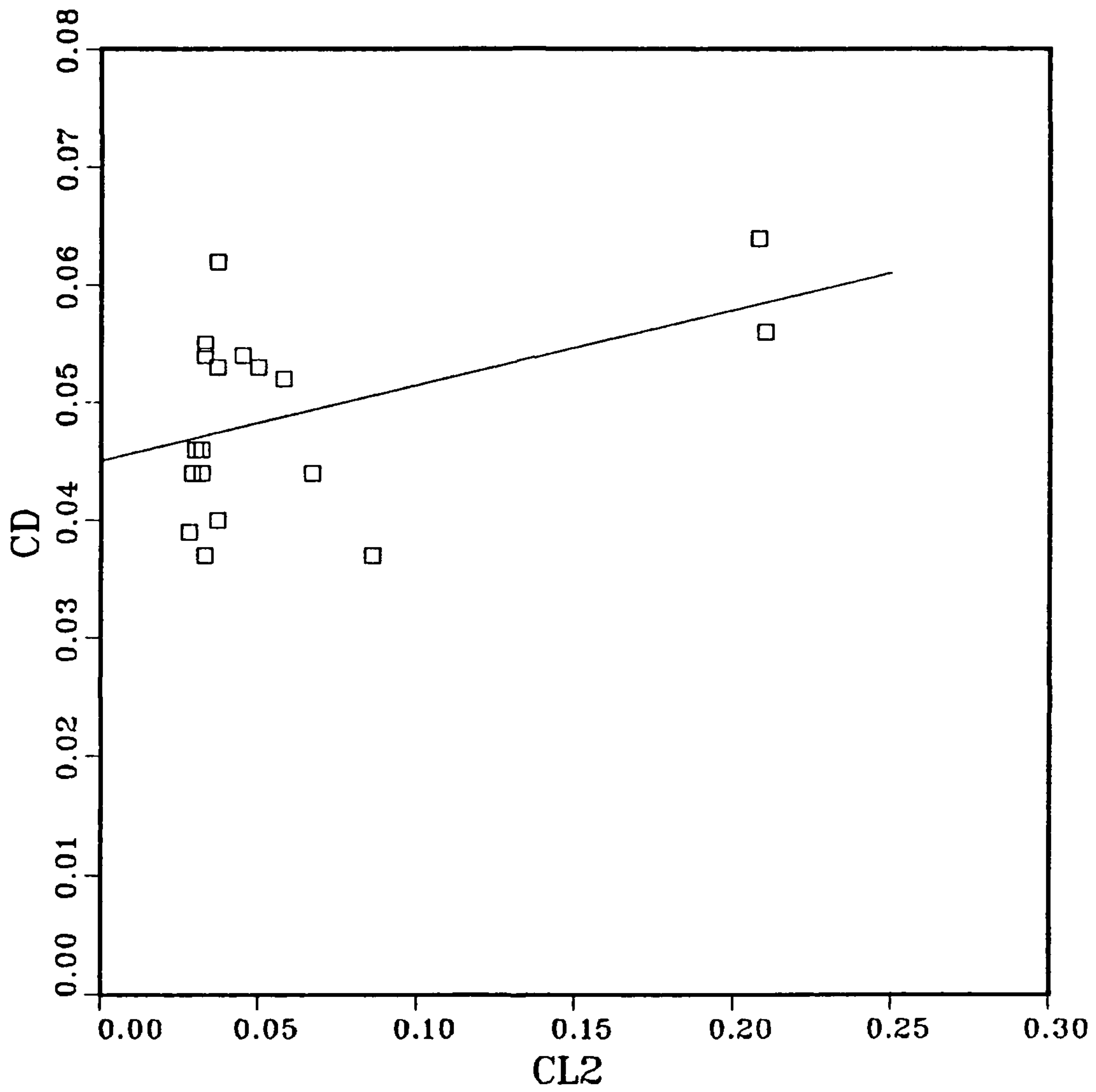

Figure 14. C_D Versus $C_L{}^2$

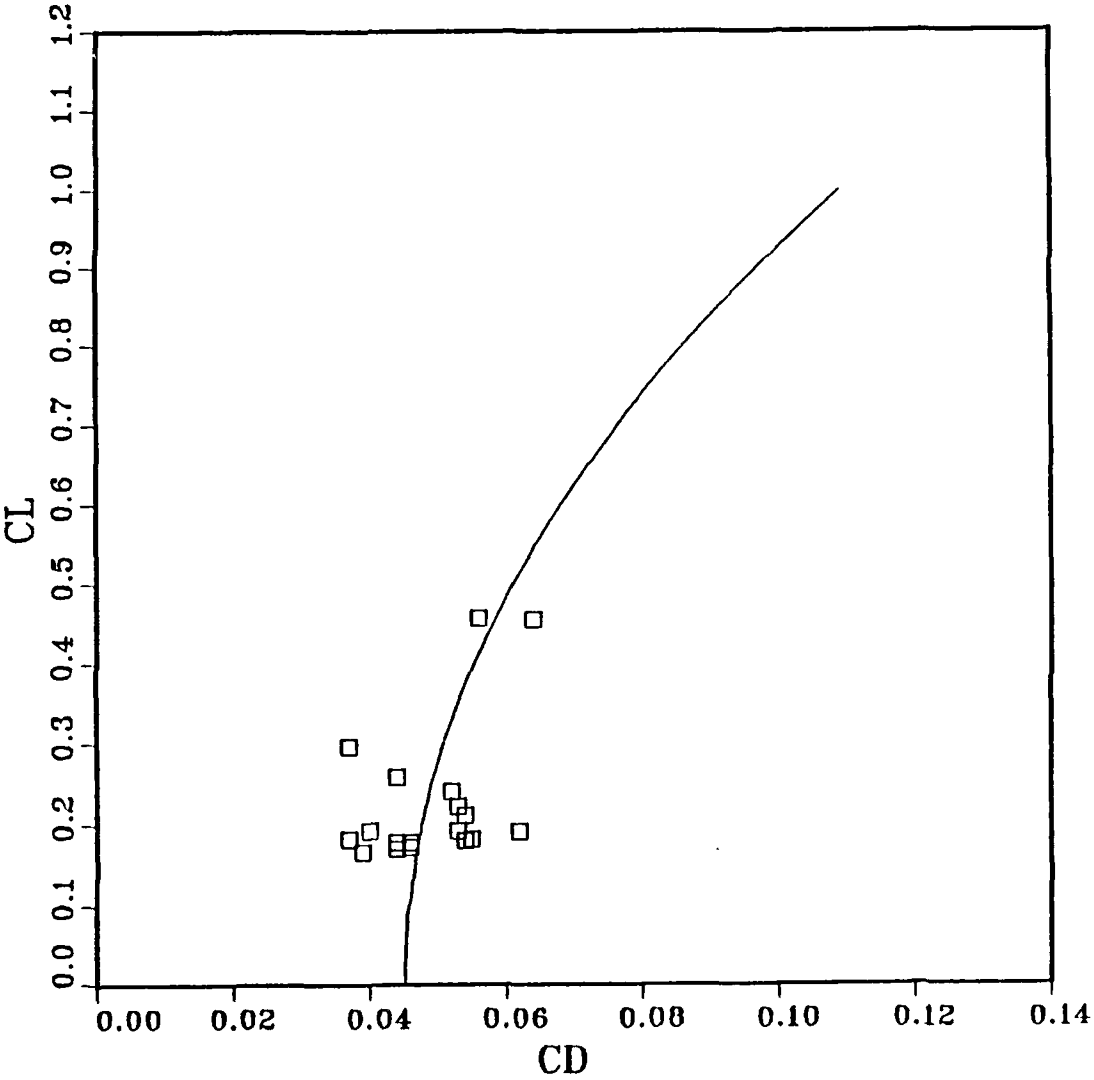

Figure 15. Drag Polar

Equation 4-5 was obtained with least square regression. The large scatter of the above two plots, raises the question of the cause of the inaccuracy. A discussion is given in Chapter V., Error Analysis. The procedure to determine the thrust required and the power required curves follows next.

From eqn. 3-6, the thrust was calculated for each velocity and the thrust required was plotted (Figure 16). For the lower part of the curve to be plotted, where no data points exist from the flight test, the use of the parabolic drag polar is practical, if only as a rough prediction. The reason that no data were obtained at that regime was lack of knowledge of the low speed behavior of the aircraft. Lower flight speeds will be investigated in later tests.

The thrust required curve gives a maximum thrust of 4.5 lbs at 110 fps velocity. The minimum thrust required can be calculated by using the drag polar, because $(C_L/C_D)_{max}$ takes place at minimum drag [Ref. 13, pp. 255-262].

From eqn. (4-5), $(C_L/C_D)_{max}$ can be estimated. This happens when

$$C_{Do} = C_L{}^2/\pi eAR$$

The above relation gives $(C_L/C_D)_{max} = 9.32$ when $C_L = 0.839$ and $C_D = 0.0901$. Then, since

$$V=(W/\tfrac{1}{2}\rho C_L S)^{1/2}$$

the velocity for $(C_L/C_D)_{max}$ can be calculated and is found to be

$$V_{(CL/CD)max} = 49.88 \text{ fps}$$

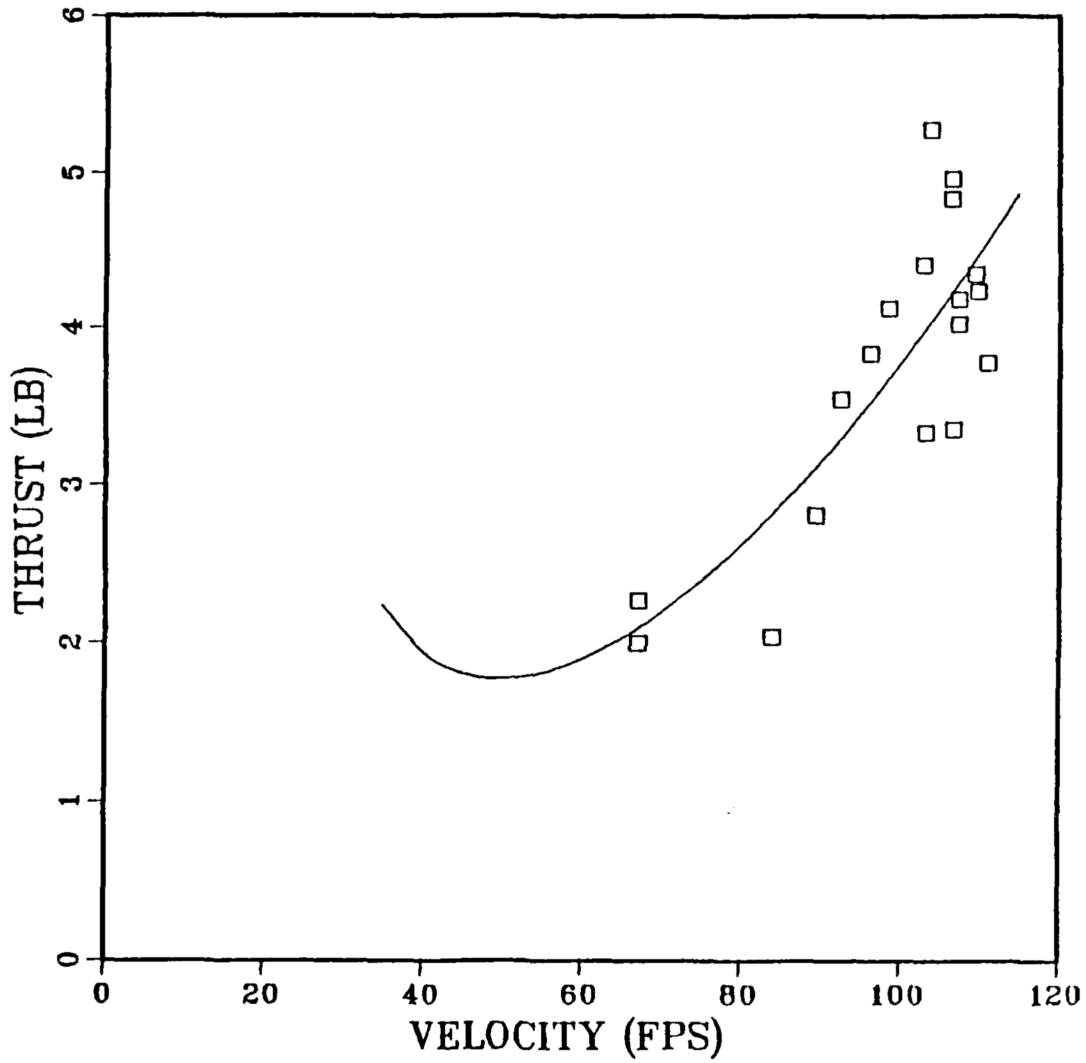

Figure 16. Thrust Required

At that velocity the minimum thrust is

$$T_{min} = 1.77 \text{ lbs}$$

Since

$$P_r = TV/550 \qquad \text{(eqn. 4-6)}$$

for each value of thrust, a corresponding power required value was calculated. To plot the power required curve, use of $P_{iw}V_{iw}$ versus V_{iw}^4 was made, which is a straight line based on the following development [Ref. 12, p. 5.12].

$$P_{iw} = DV_{iw}/550 = V_{iw}(\tfrac{1}{2}\rho V_{iw}^2 SC_D)/550 = (\tfrac{1}{2}\rho V_{iw}^3 S/550)(C_{Do} + C_L^2/\pi eAR)$$

$$= K1V_{iw}^3 + K2/V_{iw} \qquad \text{(eqn. 4-7)}$$

Therefore:

$$P_{iw}V_{iw} = K1V_{iw}^4 + K2 \qquad \text{(eqn. 4-8)}$$

which is the equation of a straight line if $P_{iw}V_{iw}$ is plotted against V_{iw}^4. By using least square regression for the data points, this equation is found to be

$$P_{iw}V_{iw} = 6.0621 + 6.2706E\text{-}7\ V_{iw}^4$$

This plot is shown in Figure 17. From this plot the power required curve can be plotted (Figure 18). To calculate the minimum power required, use of the drag polar equation was made again. Minimum power required happens when $C_L^{3/2}/C_D$ is a maximum [Ref. 12, p. 5.13], at which condition

$$C_{Do} = C_L^{2/3}/\pi eAR$$

This was found to give $(C_L^{3/2}/C_D)_{max} = 9.72$ at $C_L = 1.453$ and $C_D = 0.1801$. This high C_L value is probably unobtainable in this low Reynolds number aircraft;

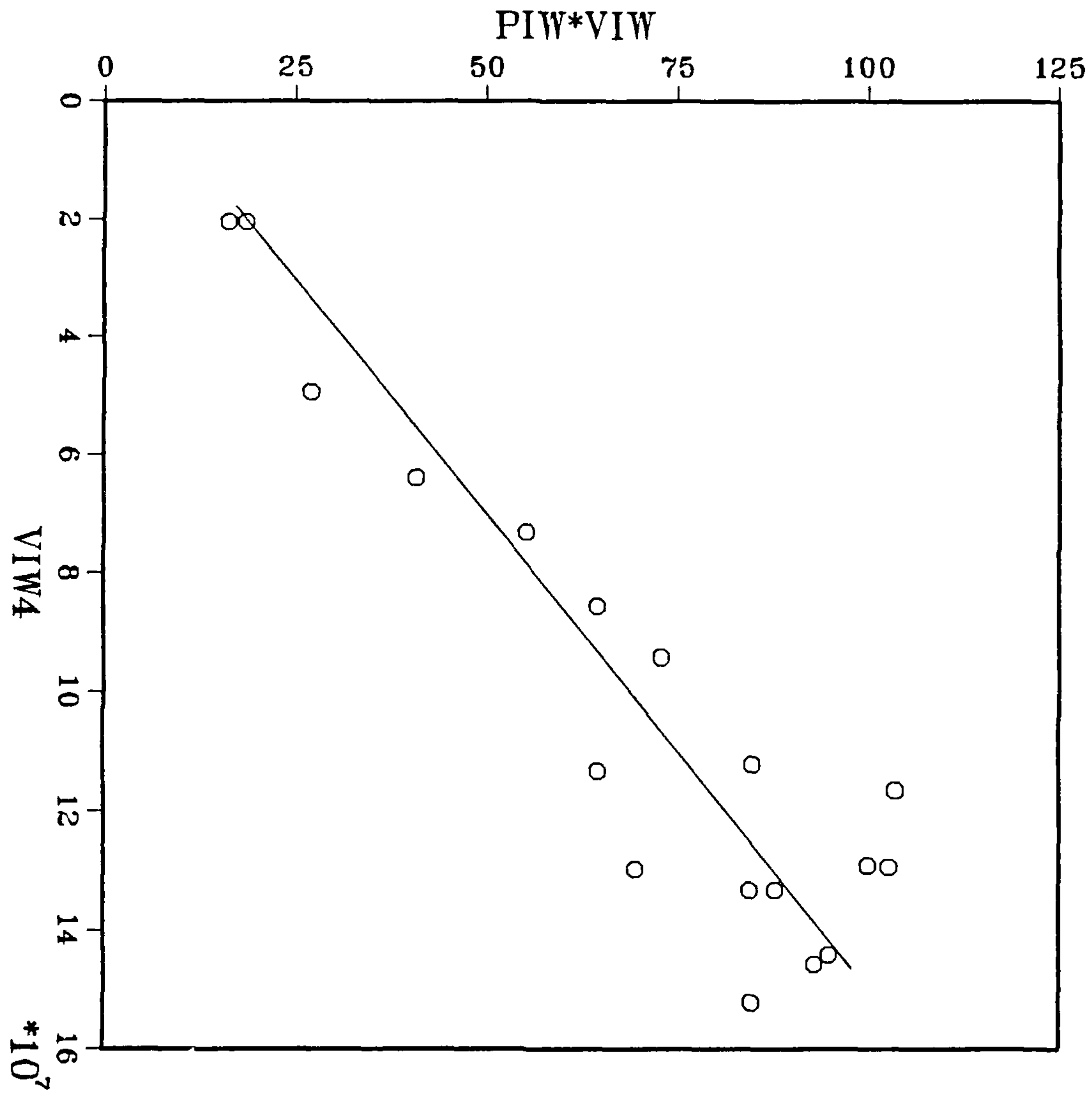

Figure 17. P_{iw} Versus V_{iw}^4

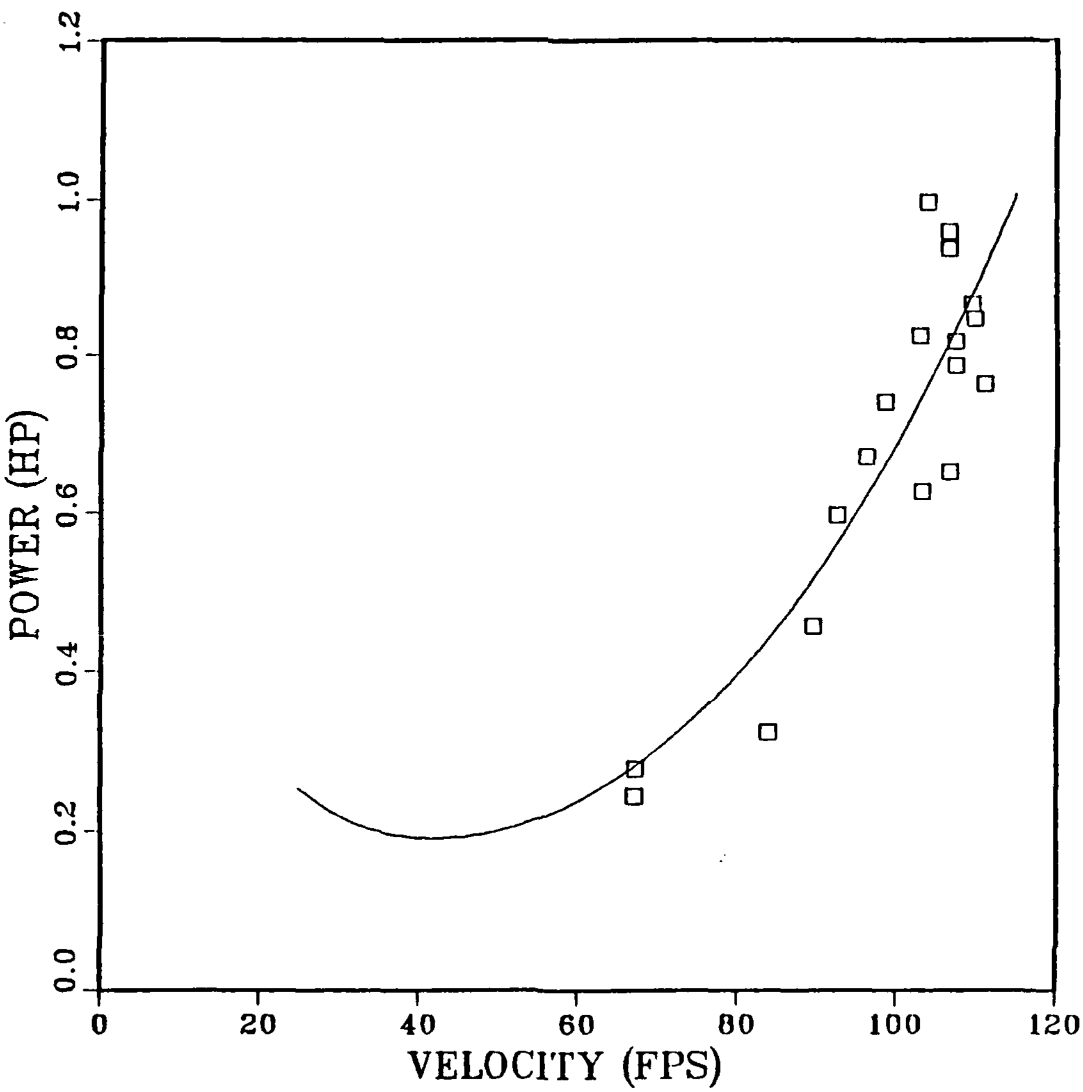

Figure 18. Power Required

probably the minimum power required value cannot be reached for steady level flight. Following the same procedure as for the thrust required, the velocity and the drag were calculated for those values. They were found to be

$V = 37.9$ fps and $D = 2.04$ lbs

Then the minimum power required from eqn. 4-9, is found to be

$P_{iwmin} = 0.216$ HP

As mentioned before, data at the lower part of the curve were not obtained due to lack of knowledge of the low speed behavior of the aircraft.

Also from the power required plot, the maximum velocity of the aircraft can be estimated at a value of about 110 fps. This happens at a maximum power required of approximately 0.85-HP. An accurate value for the maximum velocity can not be determined, because the power available curve is not known. Such should be obtained from sawtooth climb or acceleration method tests.

V. ERROR ANALYSIS

In this chapter, a discussion of the types of errors that may have occurred while collecting the experimental data will be presented, for both the Thrust and the Power methods, as defined in Chapter III. Also discussed, will be the uncertainty that these errors give to the variables that are used in development of the drag polar, the thrust required and the power required. The method that is used to obtain the results that follow, as well as sample calculations, are from Ref. 14, pp. 48-57, and can be found in Appendix D.

As described in the previous chapter, the measurements taken during the flight test were the time for each run and the RPM from the cassette recorder. Uncertainty for the time is estimated to be ±0.3 seconds and can be attributed to:

- human error by the person that was timing
- human error by the person that indicated the passage of the airplane from the beginning or the end of the run
- flight of the aircraft not absolutely straight and level
- allowance of the aircraft to drift with the crosswind

Uncertainty for the RPM is estimated to be ± 2% and can be attributed to:

- noise of the recorded signal due to engine operation and the receiver and servos

- vibrations from the engine which caused the signal to be ill-timed during playback
- actual change in the RPM during the test run
- frequency counter resolution error

To compare the effect of the ground course distance on the uncertainty of the variables, two values are given in each of the following cases: One for 1000 feet, which was the actual distance on the second day of flight testing; and one for 2000 feet, which is considered as the suggested distance.

For the velocity from V = distance/time:

uncertainties were found to be:

w_V = ± 3% for a distance of 1000 feet

w_V = ± 2% for a distance of 1500 feet

w_V = ± 1.5% for a distance of 2000 feet

For the advance ratio from J = V/Nd:

w_J = ± 3.6% for 1000 feet

w_J = ± 2.5% for 2000 feet

For the thrust coefficient from the C_T vs J plot (Figure 11):

w_{CT} = ± 52% for 1000 feet

w_{CT} = ± 33% for 2000 feet

For the thrust from $T = C_T \rho N^2 d^4$:

w_T = ± 52% for 1000 feet

w_T = ± 33% for 2000 feet

For the drag coefficient from $C_D = T/½\rho V^2S$:

$w_{CD} = \pm\ 52.7\%$ for 1000 feet

$w_{CD} = \pm\ 33\%$ for 2000 feet

For the lift coefficient from $C_L = W/½\rho V^2S$:

$w_{CL} = \pm\ 6\%$ for 1000 feet

$w_{CL} = \pm\ 3\%$ for 2000 feet

For the power required from $P_r = TV/550$:

$w_P = \pm\ 52\%$ for 1000 feet

$w_P = \pm\ 33.2\%$ for 2000 feet

The above very large values of the uncertainties give an explanation for the large scatter of the drag polar data.

By following the Power method, as described in Chapter III, to calculate the drag polar and the thrust and power required curves, smaller values of uncertainties are obtained.

Estimating a ± 1.7% uncertainty for BHP attributed to

- RPM uncertainty
- measuring device uncertainty
- reading error of the plot

the following results are obtained:

w_{CL} = same as before

w_{CD} = ±33.5% for 1000 feet

w_{CD} = ±12.5% for 2000 feet

w_T = ±32.8% for 1000 feet

w_T = ±23% for 2000 feet

w_P = ±33% for 1000 feet

w_P = ±23.2% for 2000 feet

This method gives more accurate results for C_D and T. The reason for this is that the C_T vs J plot, which is the major source of uncertainty in the Thrust method, is not used. The P_r shows the same uncertainty as in the Thrust method. The reason for this, is the use of the η vs J plot (Figure 13) at low propeller efficiency values where the curve is steep and the uncertainty of the η is large (±33%). Use of a propeller more efficient at those values of J will reduce potential errors.

Suggestions to improve the accuracy of the first flight test method are:

- The ground course distance should be increased to at least 2000 feet.
- The pilot should stay at one end of the runway so that he has a better view of the airplane's constant heading.
- A noise filter should be constructed and placed before the recorder so that the signal will be clearer.
- The recorder should be better isolated from engine vibration.

VI. CONCLUSIONS AND RECOMMENDATIONS

A. CONCLUSIONS

The purpose of this project was to develop a method to estimate the performance of a quarter-scale general aviation aircraft with minimal onboard instrumentation. In other words, the development of the drag polar and power required curves was required. As shown in the previous chapters, a method was demonstrated. The drag polar, as shown in Figure 15, was developed and the power required versus the true velocity was plotted (Figure 18). Onboard instrumentation in flight consisted of a small cassette recorder.

Three major tests were performed in order to reach the goal: the torque stand test, from which the power of two engines, the airplane engine and the electric motor, were obtained; the wind tunnel test, which was used to develop the propeller efficiency and the thrust variation with the advance ratio; and finally, the flight test, during which the velocities of the aircraft at various RPM and throttle settings were recorded.

Manipulation of the data by classical methods produced estimations for the drag polar and the power required curves. Observation of the drag polar shows a large scatter for the data points. As was explained in Chapter V, Error Analysis, this was mainly attributed to the values of the advance ratio for which the airplane flew, where a large uncertainty for the thrust coefficient exists. Also, in that regime, the propeller efficiency was found to be very low (35-45%); use of a more suitable propeller should reduce the scatter to an acceptable level.

From the drag polar, the $(C_L/C_D)_{max}$ was estimated and found to be 9.32. For those C_L and C_D values, the minimum thrust (or drag) of the airplane was calculated and found to be T_{min}=1.77 lbs at a velocity of 49.88 fps. Also, the $(C_L^{3/2}/C_D)_{max}$ was estimated and for a value of 9.72, the corresponding minimum power required was found to be 0.216 HP at a velocity of 37.9 fps.

From the power required curve, a maximum velocity of approximately 110 fps can be estimated at a maximum power required of about 0.85-HP. This corresponds to 2.6 BHP, since the propeller efficiency at that speed is only 33%.

B. RECOMMENDATIONS

In view of the above conclusions, the following recommendations are made:

1. The Aircraft

- Use of a more optimum propeller
- Use of a minimum of a 2000-foot ground test distance for future tests
- Installation of a noise filter onboard, which will give a clearer signal and will reduce the uncertainty for the RPM
- Isolating the vibration caused by the engine, by installing some special device, i.e., lord mounts. This may cause a problem with the c.g. location (which will necessitate the need for a small weight addition at the rear part of the aircraft), but it is considered a must.

- During the flight test, the pilot should stay at one end of the runway, so that he can better maintain a constant heading of the aircraft.

- Fly the airplane at lower speeds and fill in the gaps in the data.

2. The Wind Tunnel and the Torque Stand Tests

- Select a better and more accurate controller and electric motor.

- Select a more suitable mechanical scale for the torque stand.

- Use the Power method as discussed in Chapter V, Error Analysis, for data manipulation.

APPENDIX A

AIRCRAFT CHARACTERISTICS

After measuring the aircraft the following have been obtained.

Gross Weight $W = 16.5$ lbs

A/C length $l = 4.8$ ft

Wing area $S = 6.65\ ft^2$

Wing span $b = 6.94$ ft

Aspect Ratio $AR = 7.25$

Airfoil : Symmetric

Chord $c = 14.2$ in

Wing Incidence Angle $= 0.9°$

Leading edge sweep angle $\Lambda_{LE} = 1.4°$

Taper ratio $\lambda = 0.58$

Fuel weight 14 oz.

Horizontal tail area $S_{HT} = 162.3\ in^2$

Horizontal tail span $b_{HT} = 30$ in

Horizontal tail leading edge sweep angle $\Lambda_{HT} = 6.6°$

Horizontal tail taper ratio $\lambda_{HT} = 0.66$

Vertical tail area $S_{VT} = 9.95\ in^2$

Vertical tail span $b_{VT} = 9.8$ in

Vertical tail taper ratio $\lambda_{VT} = 0.32$

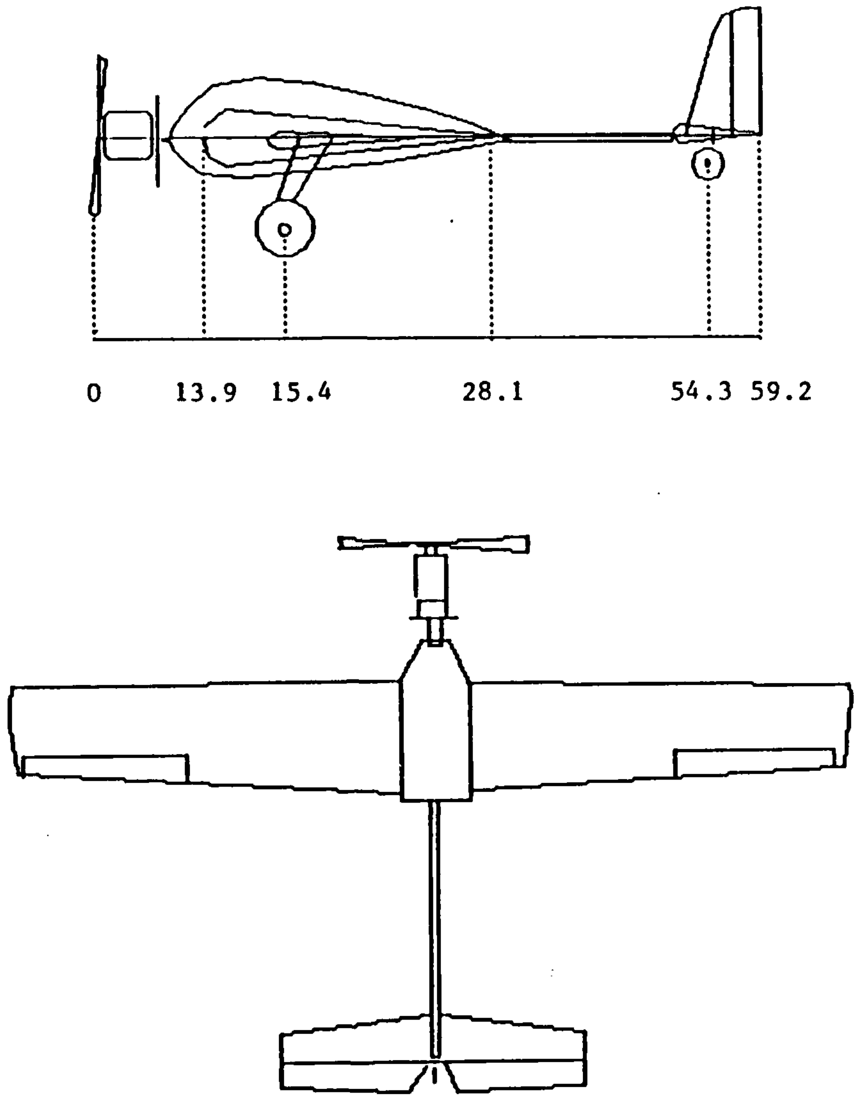

Figure 19. Top and Side View of the Aircraft

APPENDIX B

FLIGHT TEST FORM

RUN #		THROTTLE SETTING	TIME	VELOCITY RUN	VELOCITY AVG	RPM	OTHER
1	A						
	B						
2	A						
	B						
3	A						
	B						
4	A						
	B						
5	A						
	B						
6	A						
	B						
7	A						
	B						
8	A						
	B						
9	A						
	B						
10	A						
	B						

Date :
Pilot :
Temperature :
Pressure :

APPENDIX C

DATA TABLES

TABLE 1. TORQUE STAND ELECTRIC MOTOR DATA

PROP SIZE	10-7			11-8			14-8		
% THROTTLE	RPM	F (lb)	BHP	RPM	F (lb)	BHP	RPM	F (lb)	BHP
20	3670	.03	.039	3230	.03	.034	2280	.03	.024
30	5150	.04	.073	4525	.05	.080	3390	.06	.067
40	6425	.06	.137	5720	.08	.149	4425	.10	.149
50	7665	.08	.217	6870	.10	.243	5365	.14	.266
60	8830	.10	.313	8000	.14	.360	6240	.19	.413
70	9890	.12	.420	8850	.17	.512	7015	.25	.601
80	10880	.15	.578	9830	.19	.662	7760	.29	.800
90	11700	.18	.746	10550	.22	.822	8240	.33	.980
100	-	-	-	11080	.26	1.021	8600	.38	1.165

PROP SIZE	16-8			18-8			20-8		
% THROTTLE	RPM	F (lb)	BHP	RPM	F (lb)	BHP	RPM	F (lb)	BHP
20	1720	.04	.024	1490	.04	.016	1365	.04	.015
30	2715	.07	.067	2325	.07	.049	2140	.08	.053
40	3630	.13	.149	3135	.14	.140	2875	.14	.132
50	4425	.17	.266	3875	.20	.257	3520	.21	.249
60	5175	.24	.413	4455	.26	.394	4065	.28	.388
70	5920	.30	.601	5100	.33	.573	4650	.34	.543
80	6460	.36	.800	5500	.40	.770	4900	.42	.719
90	6860	.41	.980	5605	.47	.913	5100	.48	.849
100	7000	.47	1.165	6000	.52	1.105	5400	.53	1.033

TABLE 2. WIND TUNNEL DATA

THROTTLE SETTING %	VOLTAGE	V = 73.67 fps RPM	T_{read} (lb)	Tcorr (lb)	J	V = 60.06 fps RPM	T_{read} (lb)	Tcorr (lb)	J	V = 40.40 fps RPM	T_{read} (lb)	Tcorr (lb)	J
0	10	4310	-4.82	-4.82	.615	3270	-2.67	-2.67	.661	2170	-1.30	-1.30	.670
10	23	4380	-4.68	-4.68	.606	3350	-2.57	-2.57	.645	2300	-1.14	-1.14	.630
20	36	4450	-4.43	-4.46	.596	3450	-2.27	-2.30	.627	2500	-.84	-.868	.580
30	49	4585	-4.13	-4.23	.578	3665	-1.67	-1.78	.590	2815	-.14	-.245	.520
40	62	4825	-3.33	-3.33	.550	3950	.77	-.975	.547	3240	.96	.755	.450
50	75	5110	-2.33	-2.66	.519	4360	.63	.304	.496	3770	2.61	2.284	.386
60	88	5480	-0.73	-1.18	.484	4800	2.23	1.774	.450	4285	4.51	4.055	.340
70	101	5810	1.07	.480	.456	5255	4.28	3.693	.411	4790	6.76	6.173	.300
80	114	6250	3.17	2.460	.424	5650	6.58	5.875	.383	5220	8.91	8.195	.280
90	127	6290	4.37	3.550	.422	5700	8.13	7.300	.379	5330	10.76	9.935	.273
100	140	6250	5.77	5.62	.424	5700	9.23	8.350	.379	5350	10.86	9.980	.272

T = 61.9 ° F

p = 30.16 in Hg

$$\frac{\Delta p}{q} = 0.9482$$

TABLE 3. FLIGHT TEST DATA AND RESULTS

THROTTLE SETTING	V (fps)	RPM	T (lb)	C_D	C_L	BHP	P_r (HP)
5	67.170	5400	2.00	.056	.458	.640	.243
6	67.200	5450	2.27	.064	.456	.690	.277
7	83.870	6500	2.04	.037	.297	1.04	.323
8	89.420	7080	2.81	.044	.259	1.34	.457
9	92.500	7380	3.55	.052	.241	1.61	.597
10	96.180	7680	3.84	.053	.223	1.81	.671
11	98.520	7900	4.13	.054	.212	1.97	.740
12	103.18	8100	3.34	.040	.193	2.05	.627
13	102.92	8220	4.41	.053	.193	2.23	.825
14	106.73	8340	3.36	.037	.183	2.17	.652
15	103.89	8400	5.28	.062	.192	2.49	.997
16	107.43	8480	4.03	.044	.179	2.38	.787
17	107.43	8540	4.19	.046	.179	2.34	.818
18	106.60	8550	4.84	.054	.181	2.50	.938
19	109.85	8700	4.24	.044	.171	2.49	.847
20	111.05	8700	3.78	.039	.167	2.54	.763
21	109.55	8700	4.35	.046	.173	2.48	.866
23	106.64	8670	4.97	.055	.183	2.35	.960

APPENDIX D

ERROR ANALYSIS CALCULATIONS

If $Y = X_1 \bullet X_2 \text{---} X_n$

then uncertainty for Y is:

$$w_Y = [(\frac{\partial Y}{\partial X_1})^2 w_{X1}^2 + (\frac{\partial Y}{\partial X_2})^2 w_{X2}^2 + \text{---} + (\frac{\partial Y}{\partial X_n})^2 w_{Xn}^2]^{1/2}$$

where $w_{X1}, w_{X2}, \text{---} w_{Xn}$ are the uncertainties for $X_1, X_2, \text{---} X_n$

Then by estimating a .3 second error for a run with velocity 100 fps, the following calculations can be made to estimate the uncertainties using Formula 5-1.

$$V = \frac{d}{t} = 100 \text{ fps}$$

Then for a ground distance d = 1000 feet

$$\frac{dV}{dt} = \frac{d}{t^2} = -\frac{1000}{10^2} = -10$$

$$w_T = \pm .3 \text{ or } 3\%$$

$$w_V = (10)(.3) = \pm 3 \text{ or } \pm 3\%$$

For distance d = 1500 feet

$$\frac{dV}{dt} = -\frac{1500}{15^2} = -6.67$$

$$w_T = \pm .3 \text{ or } \pm 2\%$$

$$w_V = (6.67)(.3) = \pm 2 \text{ or } 2\%$$

For distance d = 2000 feet

$$\frac{dV}{dt} = -\frac{2000}{20^2} = -5$$

$w_T = \pm .3$ or $\pm 1.5\%$

$w_V = (-5)(.3) = 1.5\%$

So

For d = 1000 feet $\rightarrow w_V = 3\%$

d = 1500 feet $\rightarrow w_V = 2\%$

d = 2000 feet $\rightarrow w_V = 1.5\%$

Estimating a $\pm 2\%$ uncertainty for the revolutions of the engine, the following calculations can be made for the run with throttle setting 12. The calculations are made for distance 1000 feet. Results in parenthesis are for d = 2000 feet.

$$J = \frac{V}{Nd} = \frac{103.18}{135\ 20/12} = 0.458$$

$$\frac{\partial J}{\partial V} = \frac{1}{Nd} = .0044$$

$$\frac{\partial J}{\partial N} = -\frac{(0.6)V}{N^2} = -0.0034$$

$w_V(103.18)(.03) = 3095\ (1.548)$

$w_N = (135)(.02) = 2.7$

$w_J = [(.0044)^2(3.095)^2 + (.0034)^2(2.7)^2]^{1/2} = 0.0164(0.0114)$ or $3.6\%\ (2.5\%)$

From C_T vs J plot (Figure 11), the above values of J give a w_{CT} = 52% (33%). Then further calculations give

$T = C_T \rho N^2 d^4 = 3.34$

$$\frac{\partial T}{\partial C_T} = \rho N^2 d^4 = 334$$

$$\frac{\partial T}{\partial N} = 2C_T \rho N d^4 = .0495$$

$w_{CT} = (.01)(.52) - .0052\%(.0033)$

$w_N = (135)(.02) = 2.7$

$w_T = [(334)^2(.0052)^2 + (.0495)^2(2.7)^2]^{1/2} = 1.74\ (1.11)$ or 52% (33%)

$$C_D = \frac{T}{1/2 \rho V^2 S} = .04$$

$$\frac{\partial C_D}{\partial T} = \frac{1}{1/2 \rho V^2 S} = .012$$

$$\frac{\partial C_D}{\partial V} = -\frac{T}{1/4 \rho V^3 S} = -.00077$$

$w_T = (3.34)(.52) = 1.74\ (1.10)$

$w_v (103.18)(.03) = 3.09\ (1.55)$

$w_{CD} = [(.012)^2(1.74)^2 + (.00077)^2(3.09)^2]^{1/2} = .021(.013)$ or 52.7% (33%)

$$C_L = \frac{w}{1/2 \rho V^2 S} = .193$$

$$\frac{\partial C_L}{\partial V} = -\frac{w}{1/4 \rho V^3 S} = .0037$$

$w_V = 3.09\ (1.55)$

$w_{CL} = .0115\ (.0057)$ or 6% (3%)

$$P = \frac{TV}{550} = .627$$

$$\frac{\partial P}{\partial T} = \frac{V}{550} = .1876$$

$$\frac{\partial P}{\partial V} = \frac{T}{550} = .006$$

$$w_T = 1.74\ (1.11)$$

$$w_V = 3.09\ (1.55)$$

$$w_P = [(.1876)^2(1.74)^2 + (.006)^2(3.09)^2]^{1/2} = .33\ (.21) \text{ or } 52\%\ (33.2\%)$$

By using the Power Method as described in Chapter 5, and by estimating from the BHP vs RPM plot, a $w_{BHP} = \pm\ 1.7\%$. Also from the η vs J plot (Figure 13), the uncertainty for η is estimated to $w_\eta = \pm\ 33\%\ (23\%)$

Then,

$$P = \eta \mathrm{BHP} = .62$$

$$\frac{\partial P}{\partial BHP} = \eta = .305$$

$$\frac{\partial P}{\partial \eta} = \mathrm{BHP} = 2.05$$

$$w_{BHP} = (2.05)(0.17) = .035$$

$$w_\eta = (.305)(.33) = 1\ (.07)$$

$$w_P = [(.305)^2(.035)^2 + (2.05)^2(.1)^2]^{1/2} = .205(.144) \text{ or } 33\%\ (23.2\%)$$

$$T = \frac{P550}{V} = 3.34$$

$$\frac{\partial T}{\partial P} = \frac{550}{V} = 5.33$$

$$\frac{\partial T}{V} = -\frac{P550}{V^2} = -.032$$

$$w_P = .205\ (.144)$$

$$w_V = 3.09\ (1.55)$$

$$w_T = [(5.33)^2(.205)^2 + (.032)^2(3.09)^2]^{1/2} = 1.1(.77) \text{ or } 32.8\%\ (23\%)$$

$$C_D = \frac{T}{1/2\rho V^2 S} = .04$$

$$\frac{\partial C_D}{\partial T} = .012$$

$$\frac{\partial C_D}{\partial V} = -00077$$

$$w_T = 1.1\ (.77)$$

$$w_V = 3.09\ (1.55)$$

$$w_{CD} = [(.012)^2(1.1)^2 + (.00077)^2(3.09)^2]^{1/2} = .0134\ (.0093) \text{ or } 33.5\%(23.3\%)$$

LIST OF REFERENCES

1. Parker, H. Keith, *The Design and Initial Construction of a Composite RPV for Flight Research Applications*, Master's Thesis, Naval Postgraduate School, Monterey, California, October 1988.

2. Long, M., Model Airplanes, *National Geographic*, July 1986.

3. Hollerman, E., NASA Technical Note D-8052, *Summary of Flight Tests to Determine the Spin and Controlability Characteristics of a Remotely Piloted, Large-Scale (3/8) Fighter Airplane Model*, January 1976.

4. Duke, E., Jones, F., Roncoli, R., NASA Technical Paper 2618, *Development and Flight Test of an Experimental Maneuver Autopilot for a Highly Maneuverable Aircraft*, January 1986.

5. Coleman, R., Robins, A.J., Frary D.J., and Stephenson R., *Mini RPV Research*, August 1980.

6. Perkins, J.N. and others, North Carolina State University, Report AIAA-85-0275, *The Design and Testing of Several Joined Wing RPV's*, January 1985.

7. Bull, G., Bennett, G., *Propulsive Efficiency and Aircraft Drag Determined from Steady State Flight Test Data*, paper presented at the General Aviation Aircraft Meeting and Exposition, Wichita, Kansas, April 1985.

8. Karvinen, Cargnino, *Aircraft Propulsion Powerplants*, October 1950.

9. Sanders, Milton R., *Propeller and Engine Testing for a Mini-Remote Piloted Vehicle*, Master's Thesis, Air Force Institute of Technology, Wright-Patterson AFB, Ohio, March 1975.

10. Carson, Bernard H., *Wind Tunnel Tests of Unmanned Aircraft Propellers*, Aerospace Engineering Department, US Naval Academy, Annapolis, Maryland, Report EW-10-88, August 1988.

11. Tanner, James, *Flight Test of Half-Scale Pioneer*, Master's Thesis, Naval Postgraduate School, Monterey, California, March 1989.

12. Roberts, Sean C., *Light Aircraft Performance,* Notes, AE 4323, Naval Postgratuate School, Monterey, California, Spring 1988.

13. Anderson, John, *Introduction to Flight,* McGraw-Hill, 1985.

14. Holman, J.P., *Experimental Methods for Engineers,* McGraw Hill, 1984.

INITIAL DISTRIBUTION LIST

1.	Defense Technical Information Center Cameron Station Alexandria, Virginia 22304-6145	2
2.	Library, Code 0142 Naval Postgraduate School Monterey, California 93943-5002	2
3.	Hellenic Air Force General Staff C Branch Holargos, Attiki Greece	2
4.	Embassy of Greece Office of the Air Attache Massachussetts Avenue N.W. Washington D.C. 20008	1
5.	E. Roberts Wood, Code 67Wd Department of Aeronautical Engineering Naval Postgraduate School Monterey, California 93943	1
6.	Richard Howard, Code 67Ho Department of Aeronautical Engineering Naval Postgraduate School Monterey, California 93943	7
7.	Captain Nicolaos D. Bamichas Davaki 65, Papagou Athens, Greece	2
8.	Howard Crispin c/o Academy of Model Aeronautics 1810 Samuel Morse Drive Reston,Virginia 22090	1

9. Mr. Harry Berman 1
Naval Air Systems Command
Aircraft Division-Research and Technology
Air 931 Washington, DC 20360

10. LCDR E. Pagenkopf 1
Department of Aeronautics, Code 67Pa
Naval Postgratuate School
Monterey, California 93943-5000